COMPUTATIONAL MODELLING AND ANALYSIS OF FLOW INDUCED VIBRATIONS IN PIPING

MECH5845M Professional Project

Computational Modelling And Analysis Of Flow Induced Vibrations In Piping

Author: Bhekisipho Mpofu (201623589)

Supervisor: Prof. Harvey Thompson

Examiner:

Date: 10 August 2023

UNIVERSITY OF LEEDS

SCHOOL OF MECHANICAL ENGINEERING

MECH5845M Professional Project

TITLE OF PROJECT

Computational Modelling And Analysis Of Flow Induced Vibrations In Piping

PRESENTED BY

Bhekisipho Mpofu

201623589

If The Project Is Industrially Linked Tick This Box And Provide Details Below ☐

Company Name and Address:

This project report presents my own work and does not contain any unacknowledged work from any other sources.

Signed  Date 10 August 2023

Table of Contents

ABSTRACT

Fluid conveying pipelines form a fundamental part of modern industry. Pipework comprises a large part of many safety critical infrastructure. Flow induced vibrations, cause up to 15% of all piping failures and are responsible for over 20% of offshore oil and gas spillages. Consequently, vibration induced piping failures have resulted in large economic losses and have also had a significant environmental impact.

This project set out to develop a means of analysing flow induced vibrations in piping systems and to investigate how the vibrations can be mitigated . Firstly a critical review of the literature was done to identify the fundamental mechanisms and to review the methods that have been used to investigate the problem. The literature review showed that computational modelling is the most efficient way of investigating flow induced vibrations. It was also found that in previous studies there had been no attempt to use the finite difference method to develop a model for the computation the natural frequencies and the critical velocity.

Based on literature findings a suitable mathematical model was established. The finite difference method was then used to create model flow induced vibrations for straight pipe, clamped at both ends , with internal steady fluid flow. Using this modelling approach the critical velocities, natural frequencies and amplitude of vibration were obtained. Parametric studies were also carried out to investigate the influence of pipe and fluid physical characteristics on the stability of the system and the vibration behaviour.

The findings revealed that the finite difference method predicted the critical velocity accurately with a magnitude of error less than 1%. Thus confirming that the novel approach used is valid and reliable. The project also concluded that the susceptibility of the pipe system to vibration induced failure can be reduced by increasing the pipe flexural rigidity, reducing the ratio of fluid mass to pipe mass, reducing the support spacing and maintaining a margin from the critical flow velocity.

Acknowledgements

Firstly, I wish to express my gratitude to my project supervisor, Professor Harvey Thompson for the unwavering support, guidance and reassurance offered throughout the project. I would also like to thank Dr Hazim Hamad for the invaluable technical support.

A very special thanks goes to The Beit Trust and the University of Leeds for providing me with a scholarship to pursue my studies and thereby making this project possible.

My warmest thanks go to my wife, Kudzaiishe and my daughter, Melokuhle for being the greatest source of encouragement and motivation throughout my studies.

Finally, I thank God Most High for giving me life and all that has made this project a success.

1 Introduction

1.1 Introduction

Pipelines conveying fluids constitute a significant part of modern industry. Fluid flow is fundamental to chemical processing, power generation and transportation of essential commodities such as oil and gas. These industrial processes are safety critical because system failures can lead to the spillage of fluids which are detrimental to human health and the environment [1]. Furthermore, the failure of pipelines during operation results in economic loss [2] due to permanent loss of valuable fluid, cost of repair and lost production time. The foregoing clearly indicates the need to identify and address the root causes of failure in piping systems.

The vibration induced fatigue failure has been identified as one of the most common causes of failure in piping systems, accounting for over 15% of all piping failures in Western Europe [1,3]. The UK Government Health and Safety Executive [3] has reported that piping fatigue failure caused by vibrations has led to over 20% of oil and gas leakages in offshore operations. Consequently, the vibration of piping has become a major area of focus for pipeline designers and operators.

In many commercial applications of fluid flow the system output is directly proportional to the fluid flow rates that can be achieved. This means that operators aim to operate at the highest possible fluid flow velocities to maximise production and profits. On the other hand, high fluid velocities are associated with more severe vibrations [4,5] and consequently higher pipe failure rates. Hence it is paramount to be able to identify the safe and optimal operating ranges for a piping system.

Studies [4,5] have shown that flow induced vibrations can occur under a wide variety of flow regimes even when there is steady fluid flow without any turbulent flow or multiphase fluid flow. Vibration of pipelines conveying fluids comes about as a result of the interaction between a fluid and structural component [6]. As a result, flow induced vibrations in piping systems are influenced by the physical and structural properties of both the fluid and the pipe. This interaction brings about complex behaviour which has called for the development specialised methods and tools for the analysis of flow induced vibrations.

It has been reported [3] that one of the main design issues leading to the failure of piping is failure to have sufficient support for the pipeline leading to severe vibrations which then induced fatigue failure. This clearly shows that flow induced vibration of pipelines needs to be considered during design of piping systems as engineers need

to demonstrate that the piping systems they intend to build and operate can be operated safely.

It is evident that flow induced vibrations continue to be a cause for concern and that the mitigation of this flow induced vibrations in piping systems will lead to significant reduction in piping failure rates. The ability to predict and hence mitigate vibrations in pipelines reduces downtime, saves costs, improves safety and protects the environment.

1.2 Aim

The aim of the project was to model and analyse flow induced vibrations for a straight pipe line with fixed supports internal fluid flow using computational methods and investigate how the stability is influenced by the pipe and fluid parameters.

1.3 Objectives

To achieve this aim the following objectives were set for the project

1. Conduct a critical literature review on flow induced vibrations in piping systems
2. Develop and validate a computational model for the modelling and analysis flow induced vibrations in piping with fixed supports
3. Predict the natural frequencies of the pipe with internal fluid flow
4. Predict the critical velocity for pipe instability due to flow induced vibration
5. Predict the amplitude of vibrations
6. Conduct parametric studies to establish how the vibration characteristics and the critical velocity are influenced by pipe supports, rigidity of the pipe, pipe and fluid densities and fluid flow velocity

1.4 Report Layout

Chapter 2 presents a review of the literature which was carried out to gain an understanding of the physics of flow induced vibrations, methods that have been used to analyse the vibrations and to identify research gaps whose closure may lead to better management of the problem. Following the identification of the mechanisms and the mathematical models of flow induced vibrations, in Chapter 3 the development and verification of a finite differences based computational model for the flow induced vibrations is outlined. Chapter 4 then presents the validation of the models and the parametric studies carried out to investigate the influence of various pipe and fluid parameters on the stability of the system and the vibration characteristics. Finally, Chapter 5 presents the a summary of the main findings and the conclusions that were drawn from the project results.

2 Literature Review

2.1 Introduction

This chapter provides the fundamentals concepts of flow induced vibrations by presenting the mechanisms of flow induced vibrations and how unstable vibrations develop. The mathematical representation of the problem is also discussed. An analysis of the different approaches that have been used to investigate flow induced vibrations. Finally a brief discussion is made on some of the key findings that had relevant implications to this project.

2.2 Fluid Structure Interaction

Flow induced vibrations in piping systems come about as a result of a phenomenon called fluid-structure interaction (FSI). FSI occurs when a fluid flows inside deformable structure causing geometric changes or vibrations and then these deformations or vibrations then in turn influence the fluid flow characteristics [5,6]. As a result there is an interplay between the fluid forces and structural forces. This means that flow induced vibrations in piping are influenced by the physical parameters of both the pipe and the fluid.

Vibrations caused by fluid structure interaction are classified according to the type of fluid flow and the nature of interaction between the fluid and the structure. Figure 2.1 shows the classes of vibration mechanisms according to fluid phase type, steadiness of flow and nature of flow field.

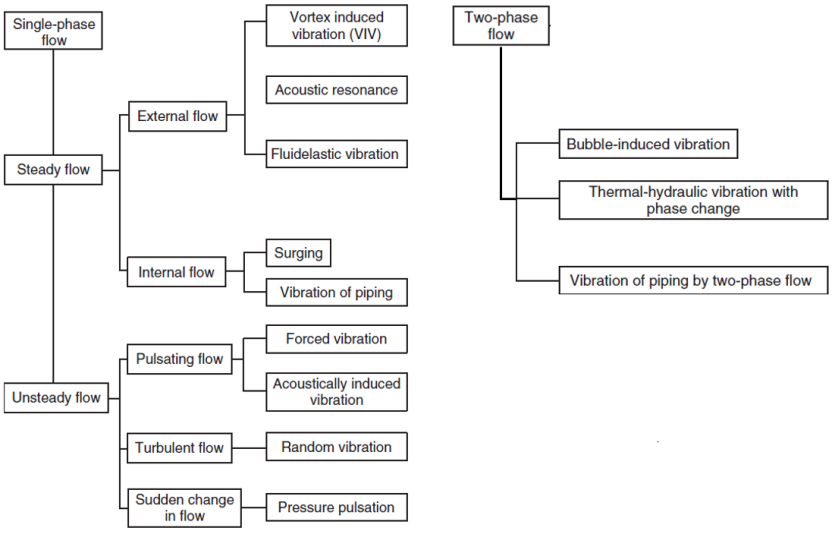

Figure 2.1 :Classification of Fluid Structure Interaction Problems [5]

It can be observed from Figure 2.1 that flow induced vibrations can occur under any type of flow even in steady flow. This means that flow induced vibrations cannot be out ruled on the basis of the type of flow since the vibrations can occur irrespective of the

type of flow. However the driving forces for the vibrations will depend on the specific mechanism of vibration [5]. In their comprehensive meta-analysis of flow induced vibrations Kaneko et al [5] pointed out that more than one mechanism of vibration may be involved in a particular case. Therefore when modelling flow induced vibrations the mechanisms of vibration have to be identified correctly so that the appropriate physical parameters can be considered in the model, otherwise the model will not be a true representation of the case under investigation.

2.3 Vibration of Pipes

Flow induced vibrations in piping conveying steady fluid flow takes the form of lateral vibrations [6] such that the vibration motion is perpendicular to the direction of the flow of fluid. In many respects, the vibration of fluid conveying piping is similar to the vibration of structural beams. The main difference is that for a fluid conveying pipe the vibrations are also affected by the stiffness of the fluid in addition to the structural stiffness. The fluid introduces a negative stiffness [4], which increases with the fluid flow velocity and affects the stability of the piping system even without an external exciting force [5] .This is the main source of complexity in the problem because it results in the vibration characteristics that change with the fluid flow velocity.

2.4 Mathematical Model of Flow Induced Vibrations

2.4.1 The equation of motion

The general equation of motion for the lateral vibrations of a pipe carrying a fluid has been derived by various researchers using two approaches namely the Hamiltonian approach and the Newtonian approach. In the Hamiltonian approach [6–9] the equations of motion are obtained by considering the kinetic energy and potential energy of the system. In the Newtonian approach [6,10] the equation of motion is derived by considering the forces and resultant motions. Both derivation approaches yield the same basic equation of motion. Given that the equation has been derived by different researchers and using two distinct methods, it can be concluded that it has been established as the standard basic model equation for flow induced lateral vibrations in straight pipelines with internal fluid flow.

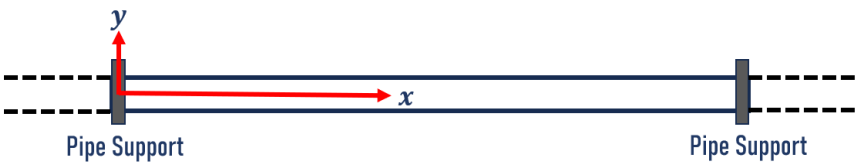

Figure 2.2 :Straight pipe system with supported ends

The equation of motion for a pipe or section of pipe held by some support systems as shown in Figure 2.2 is

$$EI\frac{\partial^4 y}{\partial x^4} + m_f V^2 \frac{\partial^2 y}{\partial x^2} + 2m_f V \frac{\partial^2 y}{\partial x \partial t} + \left(m_f + m_p\right)\frac{\partial^2 y}{\partial t^2} = 0 \qquad (2.1)$$

Where y is the lateral displacement of the pipe, E is the elastic modulus of the pipe material, I is the moment of inertia of the pipe , m_p is the mass of the pipe per unit length, m_f is the mass of the fluid per unit length, V is the mean velocity of the fluid flowing inside the pipe.

The first term in the equation,$EI\frac{\partial^4 y}{\partial x^4}$, represents the flexural restoring force. The second term, $m_f V^2 \frac{\partial^2 y}{\partial x^2}$, represents the centrifugal force due fluid flow in the curved pipe. The third term, $2m_f V \frac{\partial^2 y}{\partial x \partial t}$, represents the Coriolis forces which come about as a result of the relative motion of the pipe and the fluid. The last term, $\left(m_f + m_p\right)\frac{\partial^2 y}{\partial t^2}$, represents the inertial force of the pipe and fluid system.

2.4.2 Modelling Assumptions

In the derivation of the mathematical model the assumptions used are i) the pipe behaves like a purely elastic beam [11] meaning that the Young's Modulus is constant ii) the pipe is slender [6] which implies that the amplitude of vibration is small compared to the length, iii) the fluid flow is fully developed [6] and iv) the fluid is incompressible[6]. These assumptions help to identify the limitations of the model because once an assumption is violated the model may no longer be valid.

Although the fluid is not idealised as inviscid, the equation does not have any term with a viscosity coefficient. Païdoussis [4] has shown that the friction forces on the pipe-fluid interface ,which are caused by fluid viscosity, and the pressure loss due to the internal fluid friction, also caused by the viscosity of the fluid, cancel out each other. As a result, the viscosity dependent frictional effects do not have an influence on the vibration dynamics of the pipe. Hence there are no terms with the fluid viscosity in the equation of motion.

2.4.3 The Coriolis force term

In order to further simplify the mathematical model some researchers [10,12] have neglected the Coriolis force term totally from the equation of motion. Uduetok [10] derived the equation of motion without the Coriolis force term and used it to obtain the natural frequencies for simply supported and clamped pipes. The results obtained had a good agreement with experimental data. Yi min et al [12] also investigated the effect

of neglecting the Coriolis force in the solution of flow induced vibrations in piping systems. Figures 2.3 show the percentage error in the predicted first and second natural frequency generated by neglecting the Coriolis force term. It can be observed that for a fluid flow velocity range of 0-90 m/s the error was less than 3%. However, there was no attempt to investigate the resultant error in the predictions of critical flow velocity such a model where the Coriolis force has been neglected.

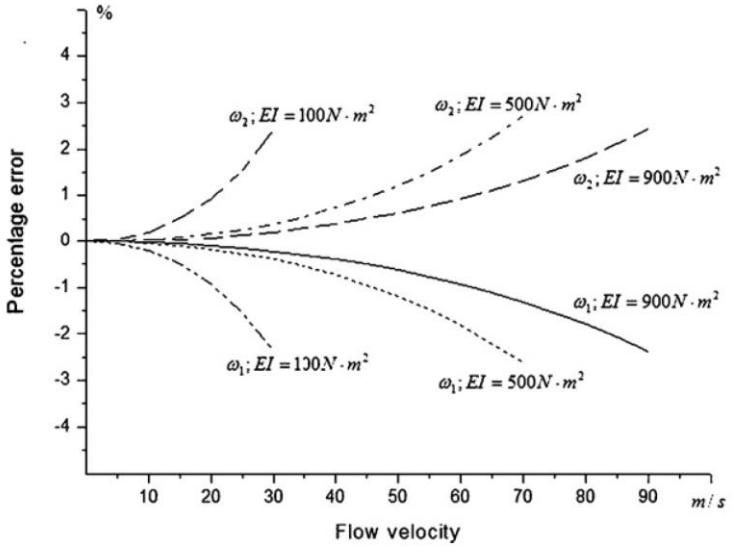

Figure 2.3 : Error magnitude in natural frequencies from model without Coriolis force term [12]

The Coriolis forces, while they have an influence on the dynamics of the pipe, do not do any actual work in the system [6]. This offers a plausible explanation for why the Coriolis forces may be neglected and only a small error is generated in the predicted natural frequency. This is significant because for many engineering applications a small magnitude of error is acceptable since safety factors are normally applied. The major advantage of a simplified model, especially in this case where the simplification involves neglecting a mixed derivative term, is that it reduces the computational effort.

2.5 Influence of pipe support type and configuration

The dynamics of the flow induced vibrations are also influenced by the type of pipe support configuration [5]. The piping support configurations fall into following major classifications: 1) both ends fixed (clamped-clamped support), 2) both ends simply supported (pinned-pinned support) ,3) one end simply supported with the other fixed (pinned-clamped), 4) one end fixed with the other free (cantilevered) [4,13]

The supports mark the boundary of the pipe domain with unique vibration characteristics and therefore the boundary conditions are determined by the support type. Since the system is modelled by a partial differential equation who solution is determined by the boundary conditions it follows that the vibration characteristics of

the pipe will be different for each type support configuration. Studies [11,13] have proven that pipe systems with the same fluid flow, pipe material, pipe span length, pipe thickness and diameter but different support types have different natural frequencies and critical velocities.

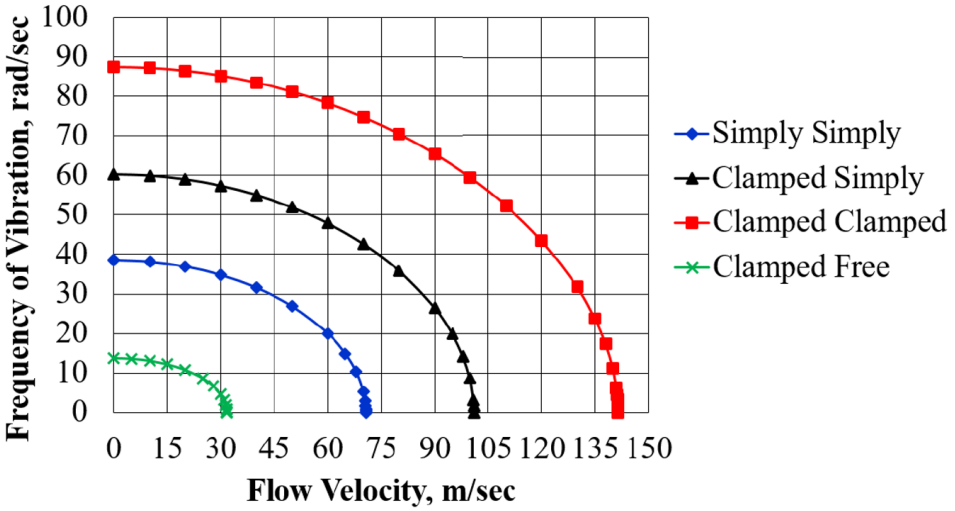

Figure 2.4 : Effect of pipe support configuration on the frequency of vibration [13]

Figure 2.4 shows that for piping systems with the same pipe and fluid parameters but different pipe end support configurations, have different frequencies of vibration at the same fluid flow velocity. Therefore demonstrating the significance of the support configuration in analysis of the flow induced vibrations.

2.6 Vibration instabilities in pipelines

The stability of a system is determined by the behaviour of the vibration amplitude. When the magnitude of vibration is constant a system is said to be undergoing stable vibrations whereas when the magnitude of vibration is growing with time the system will be undergoing unstable vibrations [14]. This implies that, while any vibration is generally undesirable for any structure, unstable vibrations are the most undesirable because they lead to large deformations and eventually failure.

The stability of piping systems with internal fluid flow has been a major point of study. Research has shown that flow induced vibrations in piping systems are stable within a finite range of flow velocity [4,5]. The fluid flow velocity where the pipe becomes unstable is known as the critical flow velocity. Two types of instabilities have been observed in flow induced vibrations namely divergence and flutter [6]. Divergence which is an instability whereby the vibration amplitude increases without oscillations as shown in Figure 2.5. On the other hand, in flutter instability the amplitude increases with oscillations as shown in Figure 2.5

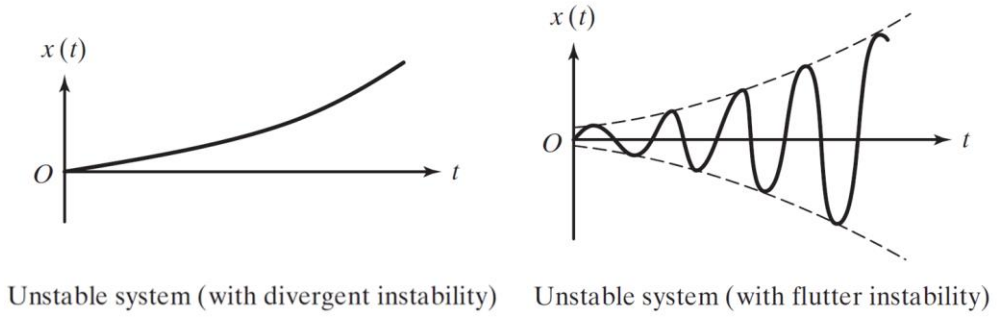

Figure 2.5 :Divergence and Flutter Instabilities [14]

A pipe with clamped ends first loses stability by divergence and then with sufficient increase in fluid flow velocity it will then transition to flutter[6]. Figure 2.6 showing the map of the instabilities plotted against a dimensionless fluid velocity parameter, u and the ratio of mass of fluid to total system mass, β, demonstrates the foregoing. The natural frequencies of the pipe system are used to determine its state of stability. the pipe first becomes unstable when the first mode natural frequency becomes zero [5]. It has also been observed that after this point the natural frequency becomes complex [6]. Therefore the fluid flow velocity which results in the first natural frequency becoming zero is the critical velocity at which the pipe becomes unstable.

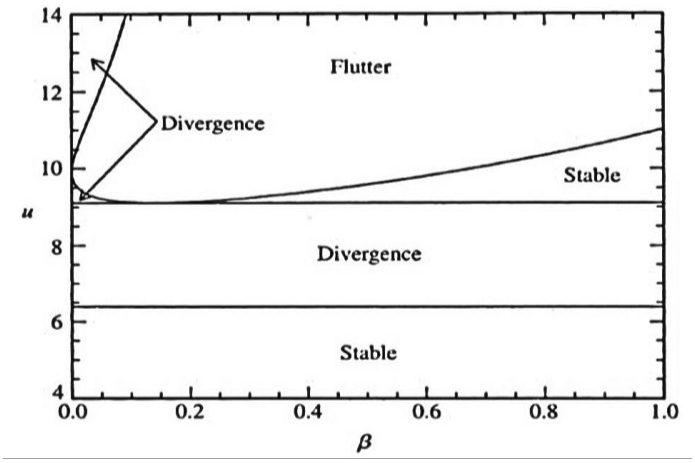

Figure 2.6 : Map of Instabilities for clamped pipes [6]

In a theoretical analysis of the physical interpretation of instabilities in flow induced vibrations, Païdoussis [6] concluded that the stability depends on the relative magnitude of the centrifugal forces and the flexural restoring forces. The centrifugal forces increase with fluid velocity. When the centrifugal forces become large enough to overcome the flexural restoring force divergence instability then take place[6]. This is significant because it provides a physical interpretation of the mechanism by which the transition from stable state to unstable state occurs.

2.7 Analysis of flow induced vibrations in piping

Various aspects of flow induced vibrations in piping systems have been studied and analysed using four classes of methods. These classes are experimental methods, analytical methods, modelling using multipurpose software packages and modelling using custom numerical methods. This section provides a summary of how these approaches been implemented and some of the key findings made.

2.7.1 Experimental approach

Experimental investigations were used in the early days of flow induced vibrations research to validate the findings which had been reached from theoretical analysis. Experimental work by Long [15] and Dodds [16] established that pipes do transition from a stable state to divergent vibration at some critical velocity and that severe vibrations can lead to permanent deformation of the pipe. In recent years experimental analysis of flow induced vibrations has typically been employed when the underlying mechanism of vibration cannot be established or when there is no access to numerical modelling tools [5] .When the underlying mechanisms are not known it is not possible to develop a mathematical model. Hence physical experimentation becomes the default option. An example of an experimental setup is shown in Figure 2.7 from a study by Khot et al [17] where the vibration data was collected using an accelerometer and the frequency response obtained using a Fast Fourier Transfer Analyser.

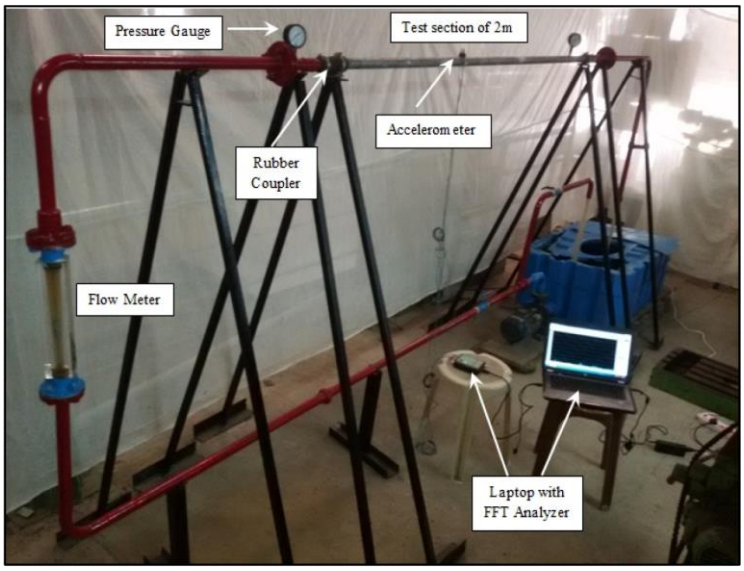

Figure 2.7 :Experimental setup for flow induced vibrations [17]

There are two particularly significant challenges with experimental analysis of flow induced vibrations. The first is that it the vibrations can become violent [6] such that beyond certain fluid velocities the error in measurements can be very large. Secondly, it has been reported that material and geometric imperfections of the particular test

pipe sections can cause the premature instability [6] which may lead to misleading conclusions about the general vibration behaviour of a whole class of pipe systems.

2.7.2 Analytical approximation approach

In one of the earliest studies on flow induced vibrations, Housner [7] adopted an analytical approach where the equation of motion for flow induced vibrations was compared with that of a vibrating beam, to derive an expression for the natural frequency of a pipe with fluid flow from the already known natural frequency of a vibrating beam. In a recent study, the analytical approach was used by Udeotok [10] to find the natural frequencies and the amplitude of vibration for simply supported and clamped pipe systems. The approach involved making simplifying assumptions to obtain simpler mathematical equations for the flow induced vibrations. These simpler equations were then solved analytically. An evident limitation of the analytical approach from these studies [7,10] is that only the first mode natural frequency could be found, whereas in practical applications a knowledge of the other higher modes may be required especially when the pipe system is connected to high-speed rotating equipment whose frequencies may excite the higher modes of vibration.

2.7.3 Commercial multipurpose packages

One of the approaches used in flow induced vibration studies[17,18] is the use of commercial multipurpose software packages. In this approach the fluid domain is solved by a fluid dynamics solver and the structural domain is solved by a structural mechanics solver [5]. In an investigation of the frequency and amplitude of vibration for a simply supported pipe, Khot et al [17] utilised ANSYS© to first solve the fluid domain and obtain the dynamic pressure. The pressure filed results obtained were then used as an input in the structural analysis of the pipe. In contrast, to the manual transfer of data between fluid and structural solver as done in the study by Khot et al [17], some commercial multipurpose packages have an inbuilt coupling between the fluid and structure solvers [5] as shown in Table 2.1

Table 2.1 : Examples of software packages used for fluid structure interaction problems [5]

Name	Fluid	Structure	Coupling
STAR-CD + NASTRAN	FVM	FEM	File
LS-DYNA	FEM	FEM	Mutual boundary
ADINA + ADINA-F	FEM	FEM	Ibid.
CFD-ACE + FEMSTRESS	FVM	FEM	Ibid.
FINAS	FEM	FEM	Ibid.

*FVM: Finite volume method, FEM: Finite element method.

The major disadvantage with the use of the commercial multipurpose packages for flow induced vibrations in piping is that the fluid solvers perform a calculation for the whole fluid domain whereas for this problem only the fluid forces acting on the structure at the interface of the pipe with the fluid are needed [6]. The calculation of forces throughout the fluid domain may be necessary and worth the cost when complex structural geometries are involved, however pipelines have simple geometries. Hence the high computational cost may not be worth the simplicity of the domain.

2.7.4 Custom numerical methods

Unlike the multipurpose solvers, the custom numerical solvers are developed specifically for the problem of flow induced vibrations. This is the approach whereby the flow induced vibrations are modelled using differential equations and then solved using numerical techniques. The literature shows this to be the most commonly used approach.

The finite element method (FEM) had been used in many studies [11,13,19–22] to investigate flow induced vibrations. A study by Mohammed et al [19] used the method to investigate the effect of having an additional spring support within the span of a simply supported pipe. in the study it was observed that the natural frequency increases nonlinearly the spring constant and that for the same spring constant the frequency varies with the location of the location of the spring along the span of the pipe. These nonlinear behaviours were also observed by Sugiyama et al [23] in their experimental study of the effect of spring supports on cantilevered pipes. This shows the finite element methods ability to deal with nonlinearities and could be one of the reasons why it has been used more widely.

Grant [20] also implemented the finite element analysis to find the vibration frequencies and subsequently the critical velocity for a uniform thickness pipe and a tapered pipe with reducing thickness. The dimensions of the tapered pipe were chosen such that the two cases had equal mass of pipe material. Interestingly, the results showed that the tapered pipe had a higher critical velocity, hence better stability, than the pipe with uniform thickness. This finding may be particularly useful for shape optimisation in some piping applications.

In a study by Lee and Park [8] the spectral element method (SEM) was used to model flow induced vibrations in piping caused by unsteady fluid flow. Another study by Lee and Oh [24] also used the spectral element method to investigate vibrations caused by steady fluid flow. In both studies [8,24] it was noted that one of the major differences between the spectral element method and the finite element method is that in the in

finite element method the pipe must be discretised into many elements whereas with the spectral element method there is no need to discretise the pipe no matter its length .This may mean that SEM has less computational cost. The forementioned difference in the discretisation requirements is not conclusive evidence that SEM has less computational requirements because the SEM also depends on the number of spectral elements used. In both the Lee and Park [8] and the Lee and Oh [24] studies, there was no investigation on the effect of the number of spectral elements on the resolution and computational cost.

The SEM was also used in study by Lee et al [25] to investigate the effect of nonlinear behaviour of the pipe material. The vibration behaviour of viscoelastic material, a viscosity coefficient, η = 250 kg/m*s, was compared to that of purely elastic material, that is with no viscous effects, η =0 kg/m*s. Figure 2.8 shows the time response of the vibration amplitude obtained from this study.

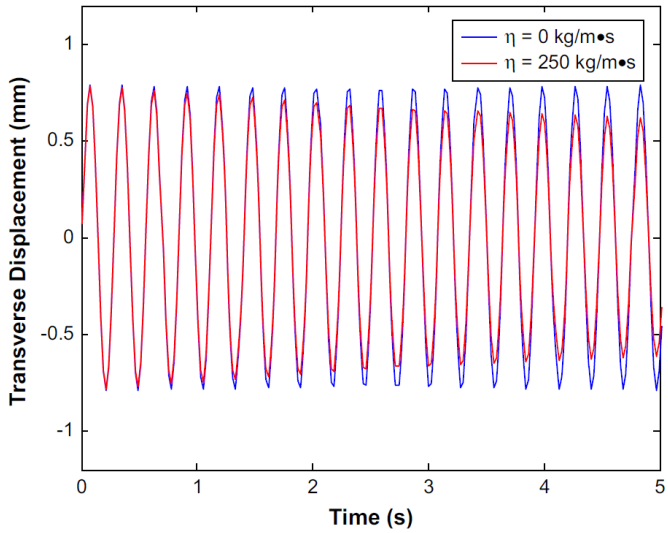

Figure 2.8 : Vibration response comparison of purely elastic and viscoelastic pipe [25]

The results presented in Figure 2.8 show that the viscoelasticity had an effect of damping the amplitude of vibration as time progressed, whereas there was negligible difference in the frequency of vibration between the two material models. Consequently, the critical flow velocity was also the same. This suggests that the damping effects of the viscoelasticity do not play a significant role on the limits of stability of a pipe with internal fluid flow since the stability is determined by the frequency.

The Galerkin method was used by Yi min et al [12] to investigate the effect of the boundary conditions on the natural frequency. The expressions for the first natural frequency derived in this study, show the order in which the natural frequency decreases. The natural frequency is highest when both ends are fixed, followed by

when one end is fixed and the other simply supported, then by the case when both end are simply supported and lastly, it is lowest for the cantilevered pipe. This ordering is consistent with the results obtained from another study [13] where the finite element method was used to calculate the natural frequencies for the same set of boundary conditions.

The finite differences method was used in a study by Gorman et al [26] to find the amplitude of vibration, hydrodynamic pressure, and flow velocities for a simply supported pipe with pulsating fluid flow. The study did not outline how the natural frequencies and critical velocities can be found using the finite difference method. The use of the finite difference method to find the natural frequencies and critical velocities was not found in the currently available literature.

2.8 Discussion and conclusion

The fundamental physics and mathematical representations of flow induced vibrations have been reviewed. The unstable vibration of pipes occurs when a specific critical velocity is exceed. This critical velocity is mutually influenced by various physical and geometric properties of the pipe and the fluid. It is therefore important to consider how these properties can be modelled when investigating flow induced vibrations.

Although the mathematical model for flow induced vibrations has mainly been used in its full form, there is evidence to suggest that the mathematical model can be simplified by neglecting the Coriolis force term without a significant compromise on the accuracy of the model. This is significant because, this eliminates the only mixed derivate terms and could mean that a wider range of methods can used to create computational models. At the same time it may be an efficient means of reducing computational cost for the commonly used methods

Direct and customised numerical modelling is the most efficient way of investigating flow induced vibrations in piping systems with steady fluid flow. In the literature this approach is more common than the experimental approach , analytical approach and use of multipurpose software packages. Amongst the methods used for direct numerical modelling of flow induced vibrations, the finite element method has been the most widely used. Although various methods have been developed implementing different numerical techniques, little attention has been given to the finite differences method.

3 Finite Difference Modelling of Flow Induced Vibrations

3.1 Introduction

This chapter describes the computational modelling of flow induced vibrations of a straight pipe with internal steady fluid flow using the finite difference method. A mathematical model is selected based on findings from the literature review. The finite difference method is then used to model the system so as to obtain the natural frequencies of vibration, the critical velocity and the vibration amplitude.

3.2 Mathematical Model

The simplified mathematical model, with the Coriolis force term neglected was selected because the model has been used to produce solutions with an error of less than 3% as highlighted in the literature review (Chapter 2). The elimination of the mixed derivative, Coriolis force term also reduces the modelling and computational effort. The equation of motion for this model is given below

$$EI\frac{\partial^4 y}{\partial x^4} + m_f V^2 \frac{\partial^2 y}{\partial x^2} + \left(m_f + m_p\right)\frac{\partial^2 y}{\partial t^2} = 0 \qquad (3.1)$$

The boundary conditions are obtained from the nature of end supports. The case investigated was that of the pipe with fixed ends as shown in Figure 3.1. This means that at each pipe support the displacement of the pipe, $y(x,t)$ is always zero. This also implies that at this point the rate of change of vibration amplitude at this point is also zero.

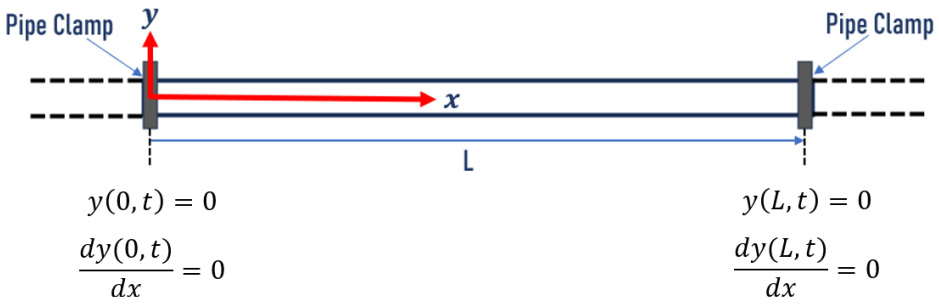

Figure 3.1 : Pipe with clamped ends showing the boundary conditions imposed by the clamps

3.3 Discretisation and Solution Approach

The finite difference method was used to represent the continuous pipe system as a discrete system. The uniform discretisation approach was used for the time and spatial domains as shown in Figure 3.2. The discrete domains constituted of a finite number of equidistant nodes. The finite difference approximations were then applied at these discrete nodes.

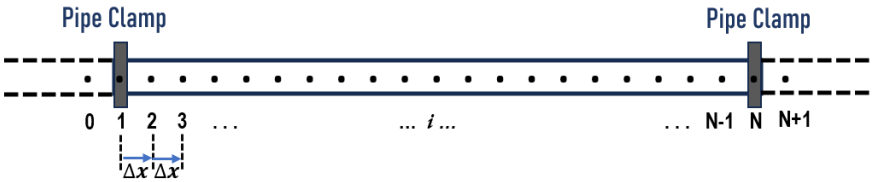

Figure 3.2 : Uniform spatial discretisation of the pipe system using nodes

The truncated Taylor series based second order centred finite difference approximations were utilized. The general expressions for the finite difference approximations to the second and fourth derivatives of a function, $f(h)$ with respect to a variable, h , with a uniform discretisation in h, are provided below

$$\frac{d^2f}{dh^2} = \frac{f_{n-1}-2f_n+f_{n+1}}{\Delta h^2} \quad (3.2)$$

$$\frac{d^4f}{dh^4} = \frac{f_{n-2}-4f_{n-1}+6f_n-4f_{n+1}+f_{n+2}}{\Delta h^4} \quad (3.3)$$

Where f_n is the approximate value of function f at node n and Δh is the node spacing.

3.4 Computation of Natural Frequency

Since the equation of motion varies in both space and time, the method of separation of variables was used, to obtain an equation in space from which the natural frequency was then computed using the finite difference method. This approach has been used successfully in the vibration analysis of other continuous systems such as solid beams[14].

Using the standard approach to separate the variables, the solution $y(x,t)$, was assumed to be a product of two functions, one function dependent only on spatial position, x and the other dependent only on the time, t such that

$$y(x,t) = Y(x)T(t) \quad (3.4)$$

The second and fourth derivatives in space and the second derivative in time were then obtained as

$$\frac{\partial^2 y}{\partial x^2} = \frac{d^2Y}{dx^2}T \quad (3.5) \qquad \frac{\partial^4 y}{\partial x^4} = \frac{d^4Y}{dx^4}T \quad (3.6) \qquad \frac{\partial^2 y}{\partial t^2} = \frac{d^2T}{dt^2}Y \quad (3.7)$$

The derivative expressions, 3.5, 3.6 and 3.7 were substituted into equation 3.1 and the resulting equation further simplified as follows

$$EI\frac{d^4Y}{dx^4}T + m_fV^2\frac{d^2Y}{dx^2}T + \left(m_f + m_p\right)\frac{d^2T}{dt^2}Y = 0$$

$$T\left(EI\frac{d^4Y}{dx^4} + m_fV^2\frac{d^2Y}{dx^2}\right) = -\left(m_f + m_p\right)Y\frac{d^2T}{dt^2}$$

$$\frac{1}{(m_f+m_p)Y}\left(EI\frac{d^4Y}{dx^4}+m_fV^2\frac{d^2Y}{dx^2}\right)=-\frac{1}{T}\frac{d^2T}{dt^2} \quad (3.8)$$

The left hand side of equation 3.3 depends only on x and the right hand side depends only on t, therefore, their common value can only be a constant.

$$\frac{1}{(m_f+m_p)Y}\left(EI\frac{d^4Y}{dx^4}+m_fV^2\frac{d^2Y}{dx^2}\right)=-\frac{1}{T}\frac{\partial^2T}{\partial t^2}=constant=\lambda \quad (3.9)$$

Two separate ordinary differential equations were then obtained from Equation 3.9, one involving x and $Y(x)$ and the other t and $T(t)$. The two equations obtained are

$$\frac{1}{(m_f+m_p)Y}\left(EI\frac{d^4Y}{dx^4}+m_fV^2\frac{d^2Y}{dx^2}\right)=\lambda \quad (3.10)$$

$$-\frac{1}{T}\frac{d^2T}{dt^2}=\lambda \quad (3.11)$$

A rearrangement of Equation 3.4 gives the following equation

$$\left(\frac{EI}{m_{tot}}\right)\frac{d^4Y}{dx^4}+\left(\frac{m_fV^2}{m_{tot}}\right)\frac{d^2Y}{dx^2}-\lambda Y=0 \quad (3.12)$$

Where $m_{tot}=m_f+m_p$

A uniform discretisation of the spatial domain was then applied. The finite difference approximations of the derivatives at the N node points of the discretised system were then applied to Equation 3.12 to obtain the following

$$\left(\frac{EI}{m_{tot}}\right)\frac{Y_{i-2}-4Y_{i-1}+6Y_i-4Y_{i+1}+Y_{i+2}}{\Delta x^4}+\left(\frac{m_fV^2}{m_{tot}}\right)\frac{Y_{i-1}-2Y_i+Y_{i+1}}{\Delta x^2}-\lambda Y_i=0 \quad (3.13)$$

Let $a=\frac{EI}{m_{tot}\Delta x^4}$ and $b=\frac{m_fV^2}{m_{tot}\Delta x^2}$ and simplifying the equation yields

$$aY_{i-2}-4aY_{i-1}+6aY_i-4aY_{i+1}+aY_{i+2}+bY_{i-1}-2bY_i+bY_{i+1}-\lambda Y_i=0$$

$$aY_{i-2}+(b-4a)Y_{i-1}+(6a-2b-\lambda)Y_i-(b-4a)Y_{i+1}+aY_{i+2}=0 \quad (3.14)$$

Letting $C_1=a$, $C_2=\mathrm{b}-4\mathrm{a}$, $C_3=6\mathrm{a}-2\mathrm{b}$, $C_4=\mathrm{b}-4\mathrm{a}$ and $C_5=a$. Equation 3.14 can then be written as

$$C_1Y_{i-2}+C_2Y_{i-1}+(C_3-\lambda)Y_i+C_4Y_{i+1}+C_5Y_{i+2}=0 \quad (3.15)$$

Equation 3.15 was applied to the node points *i=2 to i=N-1* to obtain a set of linear equations

i=2 $\quad \mathrm{C}_1Y_0+\mathrm{C}_2Y_1+(\mathrm{C}_3-\lambda)Y_2+\mathrm{C}_4Y_3+\mathrm{C}_5Y_4=0$

i=3 $\quad \mathrm{C}_1Y_1+\mathrm{C}_2Y_2+(\mathrm{C}_3-\lambda)Y_3+\mathrm{C}_4Y_4+\mathrm{C}_5Y_5=0$

i=4 $\quad \mathrm{C}_1Y_2+\mathrm{C}_2Y_3+(\mathrm{C}_3-\lambda)Y_4+\mathrm{C}_4Y_5+\mathrm{C}_5Y_6=0$

$\vdots$ $\vdots$ $\vdots$ $\vdots$

i=N-3 $\mathrm{C}_1 Y_{N-5} + \mathrm{C}_2 Y_{N-4} + (\mathrm{C}_3 - \lambda) Y_{N-3} + \mathrm{C}_4 Y_{N-2} + \mathrm{C}_5 Y_{N-1} = 0$

i=N-2 $\mathrm{C}_1 Y_{N-4} + \mathrm{C}_2 Y_{N-3} + (\mathrm{C}_3 - \lambda) Y_{N-2} + \mathrm{C}_4 Y_{N-1} + \mathrm{C}_5 Y_N = 0$

i=N-1 $\mathrm{C}_1 Y_{N-3} + \mathrm{C}_2 Y_{N-2} + (\mathrm{C}_3 - \lambda) Y_{N-1} + \mathrm{C}_4 Y_N + \mathrm{C}_5 Y_{N+1} = 0$

The boundary conditions for the clamped-clamped pipe were then applied. The boundary conditions are as follows

$$Y_1 = Y_N = 0 \tag{3.16}$$

$$\frac{dY_1}{dx} = 0 \quad \rightarrow \quad \frac{Y_2 - Y_0}{2\Delta x} = 0 \quad \rightarrow \quad Y_0 = Y_2 \tag{3.17}$$

$$\frac{dY_N}{dx} = 0 \quad \rightarrow \quad \frac{Y_{N+1} - Y_{N-1}}{2\Delta x} = 0 \quad \rightarrow \quad Y_{N+1} = Y_{N-1} \tag{3.18}$$

Equations 3.16, 3.17 and 3.18 ,obtained from the boundary conditions, were used to substitute for Y_0, Y_1, Y_{N+1} and Y_N such that the set of linear equations became

i=2 $(\mathrm{C}_1 + \mathrm{C}_3 - \lambda) Y_2 + \mathrm{C}_4 Y_3 + \mathrm{C}_5 Y_4 = 0$

i=3 $\mathrm{C}_2 Y_2 + (\mathrm{C}_3 - \lambda) Y_3 + \mathrm{C}_4 Y_4 + \mathrm{C}_5 Y_5 = 0$

i=4 $\mathrm{C}_1 Y_2 + \mathrm{C}_2 Y_3 + (\mathrm{C}_3 - \lambda) Y_4 + Y_5 + \mathrm{C}_5 Y_6 = 0$

$\vdots$ $\vdots$ $\vdots$ $\vdots$ $\vdots$

i=N-3 $\mathrm{C}_1 Y_{N-5} + \mathrm{C}_2 Y_{N-4} + (\mathrm{C}_3 - \lambda) Y_{N-3} + \mathrm{C}_4 Y_{N-2} + \mathrm{C}_5 Y_{N-1} = 0$

i=N-2 $\mathrm{C}_1 Y_{N-4} + \mathrm{C}_2 Y_{N-3} + (\mathrm{C}_3 - \lambda) Y_{N-2} + \mathrm{C}_4 Y_{N-1} = 0$

i=N-1 $\mathrm{C}_1 Y_{N-3} + \mathrm{C}_2 Y_{N-2} + (\mathrm{C}_3 + \mathrm{C}_5 - \lambda) Y_{N-1} = 0$

The foregoing set of equations were then expressed compactly in matrix vector form to give the following expression

$$\begin{bmatrix} C_1 + C_3 - \lambda & C_4 & C_5 & 0 & \cdots & \cdots & 0 \\ C_2 & C_3 - \lambda & C_4 & C_5 & 0 & \cdots & \vdots \\ C_1 & C_2 & C_3 - \lambda & C_4 & C_5 & 0 & \vdots \\ 0 & \ddots & \ddots & \ddots & \ddots & \ddots & \vdots \\ \vdots & \ddots & \ddots & \ddots & \ddots & \ddots & \vdots \\ \vdots & \ddots & \ddots & \ddots & \ddots & \cdots & 0 \\ \vdots & 0 & C_1 & C_2 & C_3 - \lambda & C_4 & C_5 \\ \vdots & \cdots & 0 & C_1 & C_2 & C_3 - \lambda & C_4 \\ 0 & \cdots & \cdots & 0 & C_1 & C_2 & C_3 + C_5 - \lambda \end{bmatrix} \begin{bmatrix} Y_2 \\ Y_3 \\ Y_3 \\ \vdots \\ \vdots \\ \vdots \\ Y_{N-3} \\ Y_{N-2} \\ Y_{N-1} \end{bmatrix} = 0$$

The matrix on the above equation is a sparse pentadiagonal square matrix of size $(N-2) \times (N-2)$ which can be expressed in the form $\boldsymbol{M} - \lambda \mathbf{I}$ where $\mathbf{I}$ is the identity matrix and $\boldsymbol{M}$ is an $(N-2) \times (N-2)$ matrix given by

$$\boldsymbol{M} = \begin{bmatrix} C_1 + C_3 & C_4 & C_5 & 0 & \cdots & \cdots & \cdots & 0 \\ C_2 & C_3 & C_4 & C_5 & 0 & \cdots & \cdots & \vdots \\ C_1 & C_2 & C_3 & C_4 & C_5 & 0 & \cdots & \vdots \\ 0 & \ddots & \ddots & \ddots & \ddots & \ddots & \ddots & \vdots \\ \vdots & \ddots & \ddots & \ddots & \ddots & \ddots & \ddots & \vdots \\ \vdots & \ddots & \ddots & \ddots & \ddots & \ddots & \ddots & 0 \\ \vdots & \cdots & 0 & C_1 & C_2 & C_3 & C_4 & C_5 \\ \vdots & \cdots & \cdots & 0 & C_1 & C_2 & C_3 & C_4 \\ 0 & \cdots & \cdots & \cdots & 0 & C_1 & C_2 & C_3 + C_5 \end{bmatrix}$$

From this it can be observed that the constant λ is the eigenvalue which is equal to ω^2, where ω is the natural frequency. The natural frequencies were found by solving the eigen value problem, $|\boldsymbol{M} - \lambda \mathbf{I}| = 0$.

$$\omega_i = \sqrt{\lambda_i} \qquad (3.19)$$

Where ω_i is the i^{th} mode natural frequency.

A MATLAB program was developed to build the matrix **M** , solve for its eigen values and calculate the 1st and 2nd natural frequencies. The MATLAB program is provided in Appendix A.

3.5 Computation of the Critical Velocity

As outline in Chapter 2, the critical velocity is the fluid flow velocity at which the pipe loses stability. This point is marked by the 1st mode real natural frequency disappearing and a development of complex natural frequencies. The critical flow velocity was computed by finding the fluid flow velocity for which the first natural frequency is zero and without any complex parts.

To optimise the search a 3 stage step reducing search algorithm was used. Starting at fluid velocity of zero the natural frequency is calculated, then the natural velocity is calculated at steps of 10m/s until a non real natural frequency was obtained. The fluid velocity where the last real natural frequency was obtained was used as the starting point for the second stage of the search. In the second stage of the search, similarly, the natural frequency was calculated at steps of 1m/s until a complex natural frequency was obtained. The velocity where the last real natural frequency was obtained was passed on to the final stage of the search. The final stage search was similar to the first two but with a step size of 0.01m/s. The last fluid flow velocity to give a real natural frequency was taken as the critical velocity. Since the last stage search was performed using steps of 0.01m/s, the critical velocity was calculated to a precision of 0.01m/s.

The search algorithm was implemented using MATLAB. The MATLAB program has been provided in Appendix B.

3.6 Computation of Pipe Displacement and Amplitude of Vibration

In the formulation, the uniform discretisation approach was used for the time and spatial domains. The time response of the displacement of the pipe from equilibrium position was obtained by applying the centred finite difference approximations in time and space to Equation 3.1 and setting up a time stepping algorithm as outlined below.

Firstly, Equation 3.1 was rearranged and the finite difference approximations applied as shown below

$$\frac{\partial^2 y}{\partial t^2} = -\frac{EI}{m_{tot}}\left(\frac{\partial^4 y}{\partial x^4}\right) - \frac{m_f V^2}{m_{tot}}\left(\frac{\partial^2 y}{\partial x^2}\right) \quad (3.20)$$

$$\frac{y_i^{j+1} - 2y_i^j + y_i^{j-1}}{\Delta t^2} = -\frac{EI}{m_{tot}}\left(\frac{y_{i+2}^j - 4y_{i+1}^j + 6y_i^j - 4y_{i-1}^j + y_{i-2}^j}{\Delta x^4}\right) - \frac{m_f V^2}{m_{tot}}\left(\frac{y_{i+1}^j - 2y_i^j + y_{i-1}^j}{\Delta x^2}\right) \quad (3.21)$$

Where y_i^j is the finite difference approximation of the displacement of pipe at spatial node *i* and time grid node *j*. The equation was further simplified to obtain the time stepping equation for the solution as follows

$$y_i^{j+1} - 2y_i^j + y_i^{j-1} = -A\left(y_{i+2}^j - 4y_{i+1}^j + 6y_i^j - 4y_{i-1}^j + y_{i-2}^j\right) - B\left(y_{i+1}^j - 2y_i^j + y_{i-1}^j\right)$$

$$y_i^{j+1} = -Ay_{i-2}^j + (4A - B)y_{i-1}^j + (2B - 6A + 2)y_i^j + (4A - B)y_{i+1}^j - Ay_{i+2}^j - y_i^{j-1} \quad (3.22)$$

Where $A = \frac{EI\Delta t^2}{m_{tot}\Delta x^4}$ and $B = \frac{m_f V^2 \Delta t^2}{m_{tot}\Delta x^2}$.

The time stepping algorithmic equation 3.22 requires initial values to start the computations. In order to initialise the computation, approximations of the displacement at the first two spatial nodes at the start of the computation (j=1), y_1^2 and y_2^2 were calculated

$$y_i^2 = -Ay_{i-2}^1 + (4A - B)y_{i-1}^1 + (2B - 6A + 2)y_i^1 + (4A - B)y_{i+1}^1 - Ay_{i+2}^1 - y_i^0 \quad (3.23)$$

$$\frac{dy(x,0)}{dt} = \frac{y_i^2 - y_i^0}{2\Delta t} \rightarrow y_i^0 = y_i^2 - 2\Delta t\frac{dy(x,0)}{dt} \rightarrow y_i^0 = y_i^2 - 2\Delta t g(x_i) \quad (3.24)$$

Where $g(x_i) = \frac{dy(x,0)}{dt}$. Substituting 3.24 into equation 3.23

$$y_i^2 = -Ay_{i-2}^1 + (4A - B)y_{i-1}^1 + (2B - 6A + 2)y_i^1 + (4A - B)y_{i+1}^1 - Ay_{i+2}^1 - y_i^2 + 2\Delta t g(x_i)$$

$$y_i^2 = \frac{1}{2}\left\{-Ay_{i-2}^1 + (4A - B)y_{i-1}^1 + (2B - 6A + 2)y_i^1 + (4A - B)y_{i+1}^1 - Ay_{i+2}^1\right\} + \Delta t g(x_i) \quad (3.25)$$

The first spatial node, i = 1 is at clamped support, therefore the boundary conditions apply

$$y_1^2 = 0$$

Equation 3.25 was then applied at the second node, i = 2 to obtain

$$y_2^2 = \frac{1}{2}\{-Ay_0^1 + (4A - B)y_1^1 + (2B - 6A + 2)y_2^1 + (4A - B)y_3^1 - Ay_4^1\} + \Delta t g(x_i) \quad (3.26)$$

The boundary conditions were then used to evaluate y_0^1

$$\frac{dy_1^1}{dx} = 0 \rightarrow \frac{y_0^1 - y_2^1}{2\Delta x} = 0 \rightarrow y_0^1 = y_2^1 \quad (3.27)$$

By substituting Equation 3.27 into Equation 3.26 the approximation for y_2^2 was then obtained as

$$y_2^2 = \frac{1}{2}\{-Ay_2^1 + (4A - B)y_1^1 + (2B - 6A + 2)y_2^1 + (4A - B)y_3^1 - Ay_4^1\} + \Delta t g(x_i)$$

$$y_2^2 = \frac{1}{2}\{(4A - B)y_1^1 + (2B - 7A + 2)y_2^1 + (4A - B)y_3^1 - Ay_4^1\} + \Delta t g(x_i) \quad (3.28)$$

Assuming first mode vibration which is symmetric about the centre of the pipe and using a similar analysis, an expression for the approximate solution at second from last node, y_{N-1}^2 was also obtained

$$y_{N_x-1}^2 = \frac{1}{2}\{-Ay_{N_x-3}^1 + (4A - B)y_{N_x-2}^1 + (2B - 7A + 2)y_{N_x-1}^1 + (4A - B)y_{N_x}^1 - Ay_4^1\} + \Delta t g(x_{N_x-1}) \quad (3.29)$$

The expression for $g(x_i)$ was derived from an analytical approximation of the displacement derived by Udoetok [10] . The first derivative of the expression with respect to time gave the expression.

$$\frac{dy(x,0)}{dt} = \omega \times \frac{16\, u_{max}(x^2L^2 - 2x^3L + x^4)}{L^4\sqrt{\left(\frac{384EI}{m_{tot}L^4} - \frac{8m_fV^2}{m_{tot}L^2}\right)}} \quad (3.30)$$

Where u_{max} is the maximum vibration velocity along the span of the pipe and ω is the frequency. The vibration frequency was computed using the FDM method described in Section 3.4.

Having obtained the initial values, time stepping through the rest of the domain could then be done to obtain the full solution. The computational algorithm was implemented in MATLAB. The MATLAB program is provided as Appendix C.

3.6.1 Stability of the displacement solution

The stability of the time stepping displacement computation program was investigated by empirical analysis. This was done by varying the combinations time step size and grid spacing and observing the stability of the solution. The variables which were

monitored in the analysis where the coefficients of the time stepping equation 3.22. The stability criteria was established from these experiments. It was found the solution became unstable when the coefficient of the y_{i-1}^{j} and y_{i+1}^{j} was less than 1. Therefore it was concluded that in order to obtain a stable solution of the pipe displacement the time step must be small enough to satisfy the following condition

$$(\Delta t)^2 \left(\frac{4EI}{m_{total}(\Delta x)^4} - \frac{m_f V^2}{(\Delta x)^2}\right) < 1 \qquad (3.31)$$

This condition was then implemented in the MATLAB program for computing the displacement as an algorithm for determining the step size such that for any given uniform spatial discretization, the minimum number of time steps required to ensure stability of the solution is determined and used for the computation. Hence the stability of solution was assured in all computations of the displacement and amplitude.

3.7 Verification of finite difference model

To verify that the finite difference model was implemented correctly, a grid convergence test and order of accuracy analysis were performed.

3.7.1 Grid Convergence

The grid convergence test was done by computing the natural frequency for a system with the following parameters taken from a study by Dangal and Ghimire [13]: Span length, L= 3.048; Young's Modulus, E= 207GPa; Moment of Inertia, I = 8.73E-09; total mass per metre, m_{tot} = 1.386 kg/m; mass of fluid per metre m_f = 0.38kg/m; V = 50m/s. The results of the test are shown in Figure 3.3

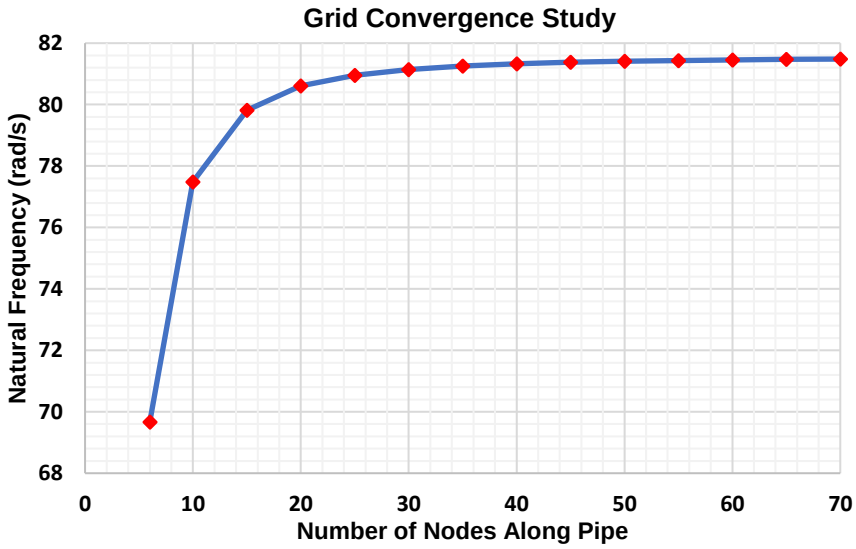

Figure 3.3 : Spatial Grid Convergence Study

The results show that as the number of nodes along the pipe section is increased, that is the node spacing is decreased, the solution converges without any observable oscillations or divergence. As shown in Figure 3.3 , the solution started to converge with 50 nodes. Further refinement of the discretisation resulted in very marginal changes.

3.7.2 Order of Accuracy

The order of accuracy was calculated by considering a sets of three node spacings defined as fine, medium and course meshes. A node spacing reduction ratio of 2 was used. For each of the three meshes, the natural frequency was calculated and the order of accuracy calculated using the following formular

$$p = \frac{ln\left(\frac{\omega_{fine}-\omega_{medium}}{\omega_{medium}-\omega_{course}}\right)}{ln\, r} \qquad (3.32)$$

Where

ω_{fine} = fine mesh solution
ω_{medium} = medium mesh solution
ω_{course} = course mesh solution
p = order of accuracy
r = node spacing reduction ratio

Table 3.1 : Results of the order of accuracy study

No of Nodes Course-Medium-Fine	$\boldsymbol{\omega_{course}}$	$\boldsymbol{\omega_{medium}}$	$\boldsymbol{\omega_{course}}$	**p**
10-20-40	77.484	80.604	81.328	2.109
20-40-80	80.604	81.328	81.500	2.071
40-80-160	81.328	81.500	81.542	2.039
80-160-320	81.500	81.542	81.552	2.024

Table 3.1 shows the results of the analysis. It was observed that the order of accuracy converges to a value of 2. This is the theoretical order of accuracy for second order finite difference approximations.

3.8 Conclusion

The finite difference method has been implemented to develop computational models for the flow induced vibrations in straight piping with clamped ends. The model verification results from the grid convergence test confirmed that the model satisfies the convergence criteria and the calculated order of accuracy converges to the theoretical value. This evidence that the computational algorithms and their implementation in the MATLAB programs are correct. Therefore it can be concluded that the finite difference model developed was successfully verified.

4 Validation of the Finite Difference Model and Parametric Studies

4.1 Introduction

In this chapter the validation process performed to check the accuracy and reliability of the finite difference model developed in Chapter 3 is presented and discussed. The validation of a computational model is performed to gain confidence that the model is a valid representation of the physics of the problem such that it can be then used to make predictions [27]. The chapter also presents the parametric studies carried out using the validated model, so as to establish the relationships between the pipe-fluid system parameter and the vibration characteristics.

4.2 Finite Difference Model Validation

The solution of the critical velocity and by extension the natural frequency of the finite difference model was validated using two methods. Firstly the results from the FDM model were compared with results from finite element analysis (FEA) studies done by Dangal and Ghimire [13]. Secondly, the dimensionless velocity parameter was calculated from the FDM model and compared with the theoretical values of the dimensionless parameters.

4.2.1 System Parameters

Three cases with different pipe materials were considered in the validation study. To enable comparison the same pipe and fluid parameters were used as in the study by Dangal and Ghimire [13]. The three materials considered were steel, aluminium and Chlorinated polyvinyl chloride (CPVC). Table 4.1 shows the system parameters.

Table 4.1 : Parameters of steel, aluminium and CPVC pipe systems conveying water

	Case 1	**Case 2**	**Case 3**
Pipe Material	Steel	Aluminium	CPVC
Support span length	3.048m	3.048m	3.048m
Young's Modulus	207 GPa	68.9 GPa	2.9 GPa
Pipe Material Density	8000 kg/m^3	2699 kg/m^3	1550 kg/m^3
Pipe Outer Diameter	25.40 mm	25.40 mm	25.40 mm
Pipe thickness	1.65 mm	1.65 mm	1.65 mm
Fluid Density	1000 kg/m^3	1000 kg/m^3	1000 kg/m^3
Mass of fluid per unit length	0.38 kg/m	0.38 kg/m	0.38 kg/m
Total mass per unit length	1.386 kg/m	0.715 kg/m	0.574 kg/m

4.2.2 Validation of Natural Frequency and Critical Velocity

The critical velocities for the above pipe-fluid systems cases were computed using the FDM model. Table 4.2 shows the results of these computations. The results were compared with the results from the Dangal and Ghimire study where the finite element method was used.

Table 4.2 : Critical Velocities of the Steel, Aluminium and CPVC pipe systems

Case	Critical Velocity (m/s)		Error
	FEA [13]	**FDM**	
Steel Pipe	141.43	142.05	0.76 %
Aluminium Pipe	81.60	81.95	0.43 %
CPVC Pipe	16.74	16.81	0.42 %

The table shows that the FDM model results differ from the FEA results by less than 1%. This shows that the FDM model has an acceptable accuracy in predicting the natural frequency and critical velocity since the results are very close to those obtained using the finite element method which has been the most widely used method for this problem.

The dimensionless critical velocity, u_c allows the comparison of results obtained from the analysis of cases with different pipe and fluid parameters. The dimensionless critical velocity is given by

$$u_c = \sqrt{\left(\frac{m_f}{EI}\right)} \times L \times V_{crit} \qquad (4.1)$$

where $m_f =$ mass of fluid/metre
$L =$ support span length
$E =$ Young's Modulus
$V_{crit} =$ critical velocity
$I =$ Moment of inertia of pipe

The theoretical dimensionless critical velocity which marks the limit of stability for pipes with clamped ends is $u_c = 2\pi$ [6]. The dimensionless critical velocity was calculated for each of the three cases using the critical velocities obtained from the FDM model and the results were compared with the theoretical value. The results of this analysis are shown in Table 4.3

Table 4.3 : Dimensionless critical velocities of the steel, aluminium and CPVC pipes

Case	Dimensionless critical velocity, u_c		Error
	Theoretical u_c	FDM u_c	
Steel Pipe	6.2831	6.2800	- 0.05%
Aluminium Pipe	6.2831	6.2798	- 0.05%
CPVC Pipe	6.2831	6.2788	- 0.07%
Average	**6.2831**	**6.2795**	**- 0.06%**

The results presented in Table 4.3 show that the FDM model underestimates the dimensionless critical velocity by 0.06%. In most practical applications this is a insignificant magnitude of error and shows that the FDM model has high accuracy in predicting the critical flow velocity. The result is also comparable to the performance of the transfer matrix method [28] where a result of $u_c = 6.283$ was obtained.

4.2.3 Validation of displacement and amplitude solution

The finite difference solution for the peak displacements was compared to the analytical approximation derived by Udoetok [10]. Case 1 (Steel Pipe Case) from Table 4.1 was used and a fluid velocity of 70m/s was used. The results for the peak displacement along the pipe section are shown in Figure 4.1

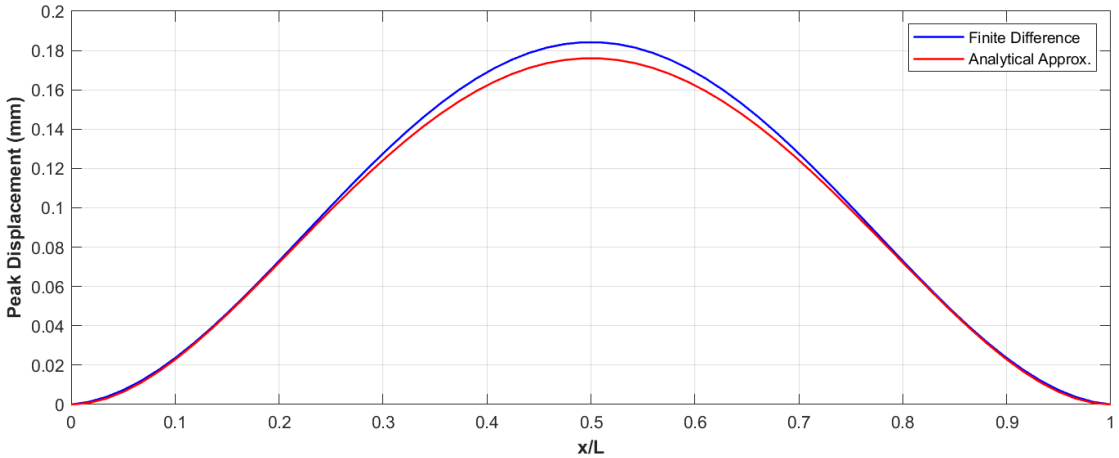

Figure 4.1 :Comparison of the FDM Model Peak Displacement Solution with the Analytical Approximation

The results show that the finite difference solution has very good agreement with the analytical approximation. The greatest difference was observed at the midspan point of the pipe where the finite difference solution gave an midspan vibration amplitude that was 4.6% greater than that of the analytical solution as shown in Figure 4.1.

4.2.4 Validation conclusion

It has been demonstrated that the FDM Model produced very accurate results for the critical velocity with errors less than 1 % for three different pipe materials covering a wide range of Young's Modulus values (2.9 GPa to 207GPa) when compared with the theoretical dimensionless parameters and widely validated finite element method results. Therefore it can be concluded that the FDM model for predicting the critical velocity and the natural frequencies was successfully validated.

The FDM solution of the pipe displacements and amplitude of vibration was also shown to be accurate, with high degree of agreement an analytical approximation model. The variance at the mid span point x/L=0.5, which is the point where the highest stresses are expected to occur under first mode vibration, was 4.6%. It was therefore concluded that the FDM model prediction of the amplitude of vibration is valid.

4.3 Parametric Studies

4.3.1 Effect of Fluid Velocity on Peak Vibration Amplitude

The effects of the fluid flow velocity on the peak vibration amplitude and the natural frequency of the system were studied by computing the natural frequencies and peak vibration amplitude over a range of fluid velocities. Figure 4.2 shows the results of the study. The first observation from the study is that as the fluid velocity is increased the natural frequency decreases with an increasing rate of decay, eventually reaching zero. This finding was expected because the fluid introduces are a negative stiffness that increases with the flow velocity and this is expected to decrease the stability decrease the stability, which is manifested by a decline in the natural frequency.

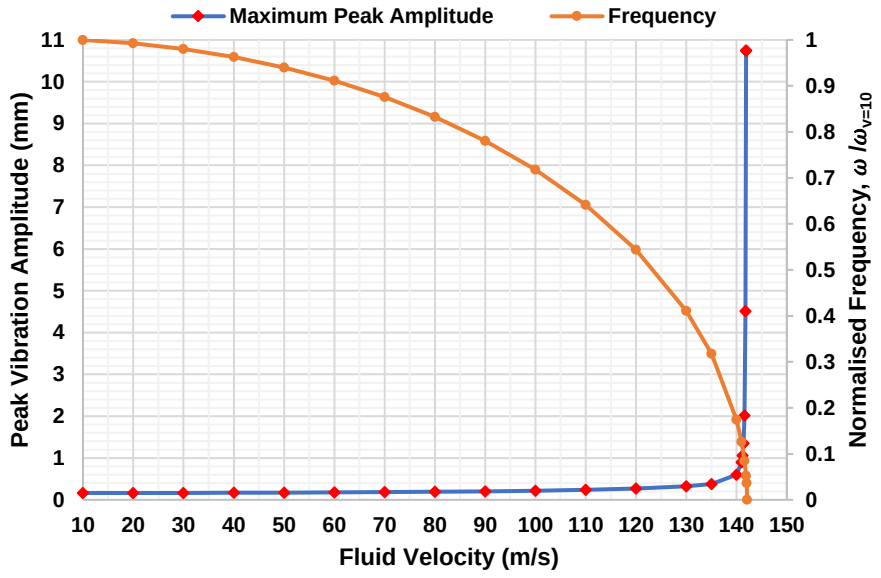

Figure 4.2 : Variation of Peak vibration amplitude and natural frequencies (normalised against the natural frequency when V=10m/s) with fluid flow velocity

Figure 4.2 also shows that there was no significant change, less than 0.2mm, in the amplitude of vibration between fluid flow of 10m/s and 135m/s. However, as the critical fluid flow velocity of 142.1 m/s was approached there was a sudden amplification in the peak vibration amplitude such that between 135 m/s and 141.9m/s the amplitude increased by a factor of 26 from 0.6mm to 10.7mm. This means severe vibrations are not only experienced when the critical velocity is exceeded but even when the fluid velocity is close to the critical velocity. These severe vibrations increase the likelihood of pipeline failure.

4.3.2 Effect of Flexural Rigidity on Critical Velocity

The flexural rigidity, EI, was varied by changing the Young's modulus while maintaining the dimensions of the pipe. Effectively this was simulating the change of rigidity by changing the material of the pipe. Simulations were performed with different values of EI ranging from 90 Nm^2 to 1800 Nm^2.The results obtained are shown in Figure 4.3

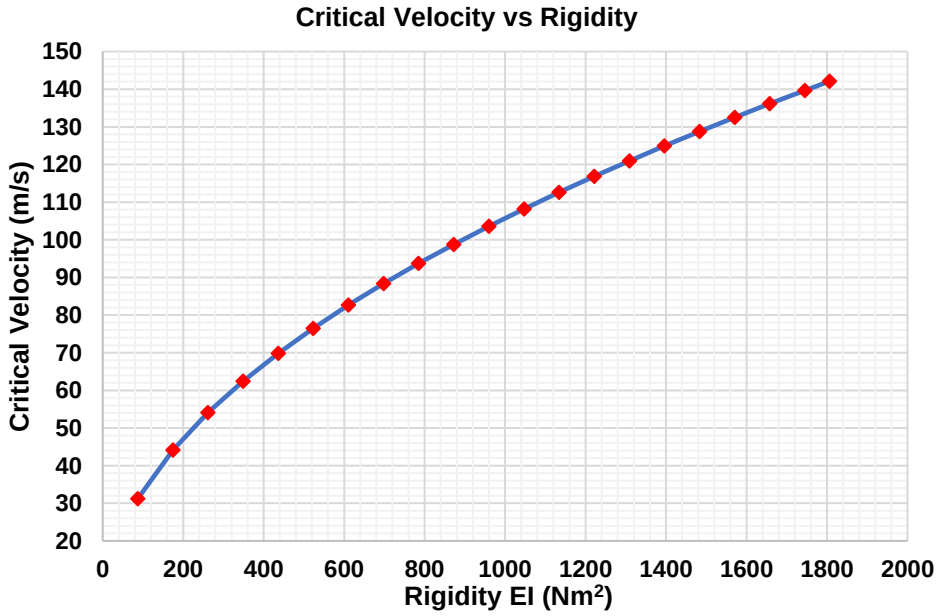

Figure 4.3 :Effect of Flexural rigidity variation on the critical velocity

Figure 4.3 shows that the critical velocity of the pipe system increases with the rigidity of the pipe. The rate of increase in critical velocity caused by increasing the flexural rigidity by 1% ranged from 0.41% to 0.50%. As outline in Chapter 2 that the pipe becomes unstable when the fluid velocity dependent centrifugal forces become large enough to overcome the flexural restoring forces. The results of the simulation have shown that as the flexural rigidity is increased, thus increasing the flexural restoring forces, higher fluid velocity is required to make the pipe unstable. Therefore the results are in agreement with theory.

4.3.3 Effect of Mass Ratio on Critical Velocity

The mass ration was varied by changing the mass of the fluid per unit length while maintaining the mass of the pipe per unit length. This was simulating the change in fluid to pipe mass ratio by changing the density of the fluid. Simulations were performed with different values of mass ration ranging from 0.05 to 0.5. A mass ratio of 0.05 means that the fluid is only 5% of the total mass of the system and similarly a mass ratio of 0.5 means that the fluid mass is 50% of the total mass of the system. Figure 4.4 shows the results obtained from this study.

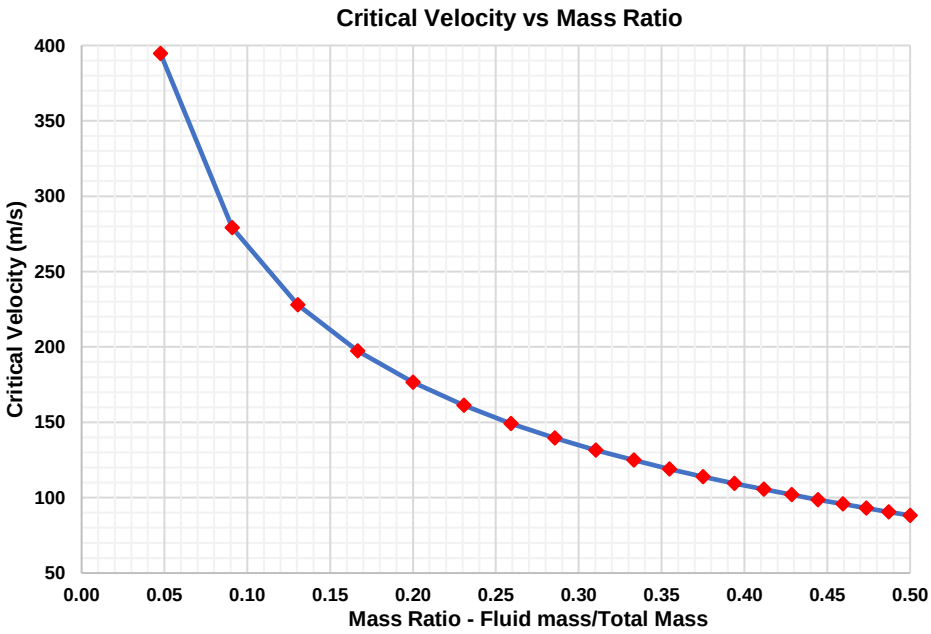

Figure 4.4 : Effect of varying the Mass Ratio (Fluid Mass: Total Mass) on the Critical Velocity

The results show that the critical velocity of decreases as the mass ratio increases. This means that as the mass of the fluid approaches the mass of the pipe, the pipe becomes less stable. This shows that the mass of the fluid has a destabilizing effect on the pipe.

4.3.4 Metamodel for the critical velocity, flexural rigidity and mass ratio

A surrogate model was developed to provide a representation of the effect of both the Flexural rigidity and the mass ratio on the critical velocity. Design of experiments was used to generate 40 sets of flexural rigidity and mass ratio values to effectively sample the flexural rigidity design range of 100 to 2000 Pa m^4 and mass ratio design range of 0.05 to 0.50. The critical velocities for these sets of design points were then computed. The results of the simulation were then used to generate a metamodel using a MATLAB program provided by the project supervisor, Prof Harvey Thompson. Figure 4.5 shows the response surface. The simulation results used to generate the metamodel are provided in Appendix E.

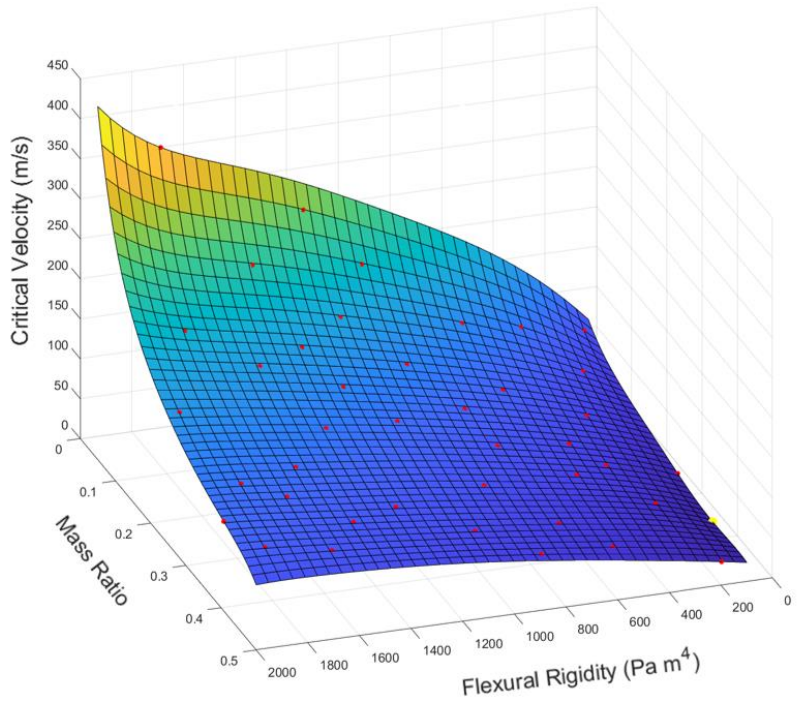

Figure 4.5 : Surrogate Model Representing the critical velocity response in the flexural rigidity and mass ratio (mass of fluid/total system mass) design space

The model shows that the critical velocity is lowest and pipe is least stable when the mass ratio is large and the flexural rigidity is small. A large mass ratio means the relative mass of the fluid is large hence the destabilising centrifugal forces are also relatively high, thereby resulting in a low critical velocity. The model gives a good representation of how the two design variables simultaneously affect the critical velocity.

4.3.5 Effect of pipe clamp spacing on Critical Velocity

The effect of the pipe clamp spacing on the critical velocity was studied for two different pipe materials, steel and aluminium, with two different fluids, water and oil. Four cases were studied 1) Steel pipe with water 2) Steel Pipe with Oil 3) Aluminium Pipe with water and 4) Aluminium pipe with oil. The pipe material and fluid properties are given in Table 4.4.

Table 4.4 : Pipe and Fluid Parameters for the pipe clamp spacing study

Steel	Young's Modulus	207 GPA
	Density	8000 kg/m^3
Aluminium	Young's Modulus	68.9 GPA
	Density	2700 kg/m^3
Water	Density	1000 kg/m^3
Oil	Density	800 kg/m^3

The critical velocity was computed for different pipe clamp spacing length starting from 1metre to 6metres, which corresponded to 39 times and 236 times the outer diameter of the pipe respectively. The results for this analysis are shown in Figure 4.6

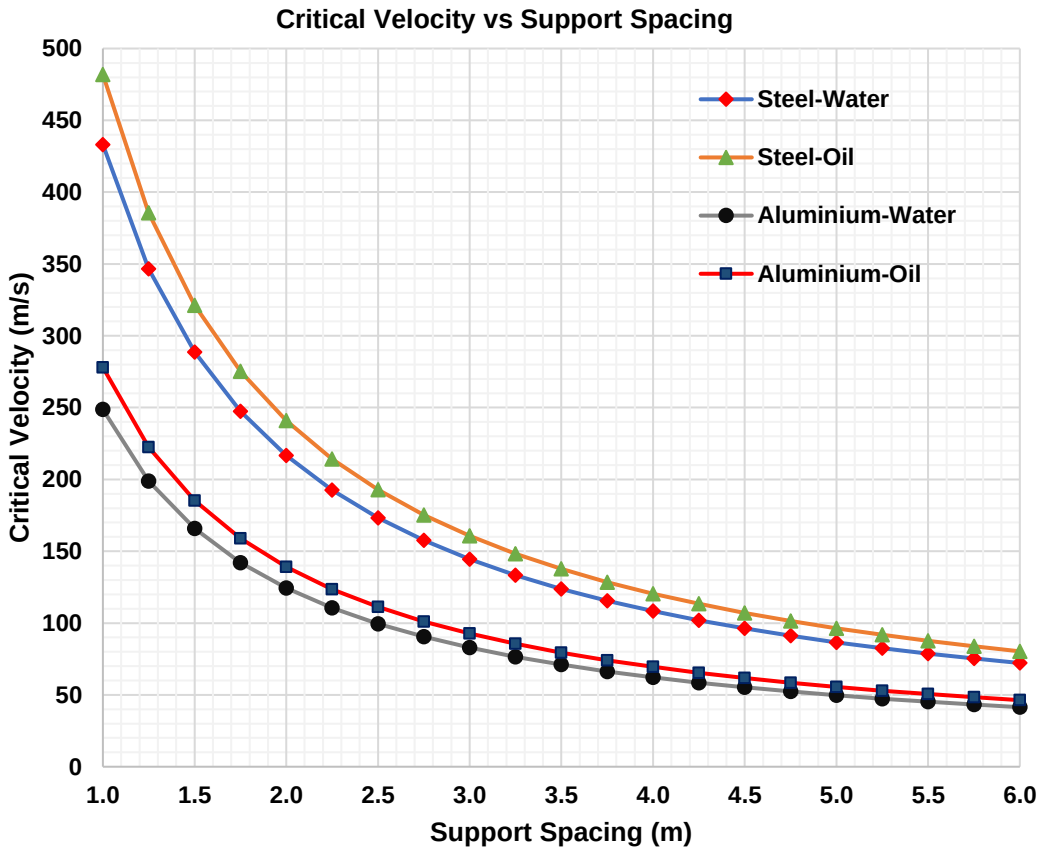

Figure 4.6 : Effect of clamp (support) spacing on the critical velocity for four different pipe material and fluid type combinations

Figure 4.6 shows that the critical velocity value decreases with an increase in the support spacing. This was expected because reducing the pipe spacing means adding more supports to the system, hence it is expected that with more supports the pipes becomes more stable and thus have a higher critical velocity. This finding agrees with the results of the study by Ugochukwu et al[21].

Figure 4.6 also shows that at each supporting spacing the highest critical velocity is obtained with steel-oil pipe system, followed by the steel-water system, then the aluminium-oil system and lastly the aluminium water system. It can be observed that for both materials the denser fluid gave a lower critical velocity. By considering the mathematical model, it can be observed that the fluid density is directly proportional to the centrifugal force term, $m_f V^2 \frac{\partial^2 y}{\partial x^2}$. As a result, with a larger fluid density the centrifugal forces become large enough to overcome the flexural restoring forces at a

lower fluid velocity than with a smaller fluid density. Therefore, the results are consistent with theory.

The results also show that as the support span length increases the difference in the critical velocity for the four cases becomes less marked. At a span length of 1m the difference between the highest and lowest critical velocities of the 4 cases is 233m/s whereas at a span length of 6m the difference is 39m/s. This implies that as the span length increases the pipe material density, pipe material Young's modulus and fluid density become less significant to the stability of the system. Therefore, in a piping system with relatively large support span length, it may not be an effective approach to attempt to improve the stability limit by changing the pipe material. The solution will depend on a case-by-case basis as there are other factors to be considered such as the pipe and support material costs.

4.3.6 Conclusion

This project set out to investigate the relationship between the physical properties of the system and the critical velocity and vibration characteristics.

It has been established that the fluid flow velocity does not have a large influence on the vibration amplitude when it is not close to the critical point. An inflection of this behaviour occurs close to the critical flow velocity where small increases in the flow velocity start to have a large impact on the amplitude of vibration. The investigation also confirmed that as fluid flow velocity increases the fundamental frequency of the system decreases until it vanishes.

The findings have also clearly indicated that the ratio of fluid mass to total system mass has an inverse influence on the critical velocity. On the other hand the flexural rigidity has a direct relationship with the critical velocity.

The investigations have also shown that the pipe support spacing has an inverse relationship with the critical velocity. An interesting observation from the study of the influence of pipe supports on two different metals, was that for the same fluid, the lighter metal (aluminium) requires smaller supports spacing and hence more supports than the heavier metal (steel). On the other hand if the system weight is used as criteria for determining the number of supports the opposite conclusion will be reached as the heavier metal will need more supports. This shows that in the design of piping systems a wholistic approach needs to be taken which also takes into account the systems susceptibility to flow induced vibrations.

5 Conclusion

This chapter outlines the achievements realised from the project. A discussion of some of the key findings is also done, including the limitations. Finally a conclusion on the project is made and recommendations for future work provided.

5.1 Achievements

- A research methodology gap was identified from the literature review
- An accurate computational model was developed using the finite difference approach, for the computation of the natural frequency and subsequently the critical velocity of a straight pipe conveying steady fluid flow. This is a novel approach to the problem which has not been reported in the available literature.
- The model for calculation of the vibration amplitude was also developed using the finite different approach
- The relationship between the fluid flow velocity and the natural frequencies and amplitude of vibration was established through parametric studies
- The effects of the flexural rigidity, ratio of fluid mass and to total mass and spacing of clamped supports on the critical velocities were also established. A surrogate model was developed for determining the critical velocities for a flexural rigidity and mass ratio design space

5.2 Discussion

The implementation of the finite difference method in this project was made possible by adopting a mathematical model for the flow induced vibrations where the mixed derivative Coriolis force term was neglected. This allowed the separation of variables to be performed and consequently the finite difference method to be used to calculate the natural frequency and the critical velocity. In most of the studies reported in literature, the equation with the mixed derivative Coriolis force term is used. This could explain why the finite differences method, although simpler to implement, had not been used to find the natural frequencies and critical velocity. Surprisingly, the results obtained in this project have shown that when the Coriolis force term is neglected and the finite difference method the critical velocity to a negligible magnitude of error.

One of the key findings was that as the flow velocity approaches the critical point there is a substantial increase in the amplitude of vibration. This implies that that there is a proportionate increase in the cyclic stresses experienced by the pipe. From theory of fatigue life, the effect of this would be to reduce the number of cycles that the pipe can endure before it undergoes fatigue failure. Therefore, during the operation of a pipeline

an appropriate margin from the actual critical velocity needs to be chosen to mitigate fatigue failure and maximise the life of the pipe.

One of the limitations of the finite difference model is that it likely to produce inaccurate results for piping systems with a short support span length, because as the span is reduced the slenderness of the system may be decreased to an extent that the slenderness condition is violated and the mathematical model becomes invalid. The model also assumes that the pipe will only behave in a purely elastic manner. However for weaker material such as plastics, large vibrations which cause plastic deformation can occur as shown in experimental studies reported in the literature. Therefore, the results need to be applied to plastic materials with due consideration.

In the design spaces explored the critical velocities in some cases were found to very high exceeding 300m/s. This was the case when the fluid to total mass ratio is very small. One of the conditions which can cause low mass ratio is when the fluid conveyed is a gas. Now when gases travel at such high velocities they become compressible. This then violates the assumption made in the derivations of the equations of motion that the fluid is incompressible. Therefore, care must be taken to confirm the compressibility of the fluid at the computed critical velocity before it is accepted as valid. This can be done by calculating the Mach number for the specific fluid and ensuring that it is incompressibility limit is not exceeded.

5.3 Conclusions

The finite difference method is applicable to modelling and analysis of flow induced vibration problems. Although its application is only possible in the absence of the mixed derivative Coriolis force term, it still yields accurate results which are comparable to established methods and are consistent with theory.

To reduce vibration induced failures in clamped piping systems, the stability of a fluid conveying pipe system can be improved by any of the following system modifications 1) maintaining a margin of safety from the critical velocity 2) increasing the flexural rigidity, which can be achieved by using a pipe with a higher Young's Modulus, 3) decreasing the fluid mass to pipe mass ratio which can be achieved by using a denser pipe or lighter fluid and 4) decreasing the spacing between clamps.

5.4 Future work

Further investigation into the inclusion of non linear material models such as viscoelastic models the with the finite difference model which has been developed is needed so as to broaden the scope of problems on which it can be applied.

References

1. Keprate A, Chandima Ratnayake RM, Sankararaman S. Minimizing hydrocarbon release from offshore piping by performing probabilistic fatigue life assessment. Process Safety and Environmental Protection. 2017 Feb;106:34–51.

2. Guidelines for the Avoidance of Vibration Induced Fatigue Failure in Process Pipework. London: Energy Institute; 2008.

3. McGillivray A, Hare J. Offshore hydrocarbon releases 2001-2008 [Online]. Health and Safety Executive 2008; 2008. Report No.: RR672. [Accessed 2 February 2023] Available from: https://www.hse.gov.uk/research/rrhtm/rr672.htm

4. Paidoussis MP. The canonical problem of the fluid-conveying pipe and radiation of the knowledge gained to other dynamics problems across Applied Mechanics. *Journal of Sound and Vibration*. 2008 Feb;310(3):462–92.

5. Kaneko S, editor. *Flow-induced vibrations: classifications and lessons from practical experiences.* 1st ed. Amsterdam ; Oxford: Elsevier; 2008. 284 p.

6. Paidoussis MP. *Pipes Conveying Fluid: Linear Dynamics I. In: Fluid-Structure Interactions* [Online]. Elsevier; 2014 [Accessed 2 February 2023]. p. 63–233. Available from: https://linkinghub.elsevier.com/retrieve/pii/B978012397312200003X

7. Housner GW. Bending Vibrations of a Pipe Line Containing Flowing Fluid. *Journal of Applied Mechanics.* 1952 Jun;19(2):205–8.

8. Lee U, Park J. Spectral element modelling and analysis of a pipeline conveying internal unsteady fluid. *Journal of Fluids and Structures*. 2006 Feb;22(2):273–92.

9. Chen Z, Han K, Ren F, Zhu W, Lu K, Yang H, et al. Influence of transverse vibration induced by fluid-structure interaction on pipeline strength. *Nuclear Engineering and Design.* 2023 Sep;411(112445):1–9.

10. Udoetok ES. Internal Fluid Flow Induced Vibration of Pipes. *Journal of Mechanical Design and Vibration*. 2018;6(1):1–8.

11. Olson LG, Jamison D. Application Of A General Purpose Finite Element Method To Elastic Pipes Conveying Fluid. *Journal of Fluids and Structures*. 1997 Feb;11(2):207–22.

12. Yi-min H, Yong-shou L, Bao-hui L, Yan-jiang L, Zhu-feng Y. Natural frequency analysis of fluid conveying pipeline with different boundary conditions. *Nuclear Engineering and Design.* 2010 Mar;240(3):461–7.

13. Dangal M, Ghimire SK. Modeling and Analysis of Flow Induced Vibration in Pipes Using Finite Element Approach. *Proceedings of IOE Graduate Conference*, 2019-Summer. 2019 May;6:725–32.

14. Rao SS. *Mechanical vibrations*. 5th ed. Upper Saddle River, N.J: Prentice Hall; 2011. 1084 p.

15. Long RH. Experimental and Theoretical Study of Transverse Vibration of a Tube Containing Flowing Fluid. *Journal of Applied Mechanics*. 1955 Mar 1;22(1):65–8.

16. Dodds H, Station L. Effect of High-Velocity Fluid Flow on the Bending Vibrations and Static Divergence of a Simply Supported Pipe [Online]. Washington: National Aeronautics And Space Administration; 1965 Jun [Accessed 3 May 2023]. Available from: https://apps.dtic.mil/sti/citations/ADA393464

17. Khot SM, Khaire P, Naik AS. Experimental and simulation study of flow induced vibration through straight pipes. In: *2017 International Conference on Nascent Technologies in Engineering (ICNTE)* [Online]. Vashi, Navi Mumbai, India: IEEE; 2017. p. 1–6. [Accessed 2 Nov 2023] Available from: http://ieeexplore.ieee.org/document/7947938/

18. Qu W, Zhang H, Li W, Sun W, Zhao L, Ning H. Influence of Support Stiffness on Dynamic Characteristics of the Hydraulic Pipe Subjected to Basic Vibration. *Shock and Vibration.* 2018 Nov 18;2018:1–8.

19. Mohamed JA, Mohammed Q, Hatem R. Stability Analysis of Pipe Conveying Fluid Stiffened by Linear Stiffness. International *Journal of Current Engineering and Technology.* 2016 Aug;6(5):1764–9.

20. Grant I. Flow Induced Vibrations In Pipes, A Finite Element Approach [Online]. Cleveland State University; 2010 [Accessed 11 February 2023]. Available from: https://engagedscholarship.csuohio.edu/etdarchive/633

21. Ugochukwu O, Onyenobi EGI, Chinwendu S. Analysis of the Effects of Pipe Specifications on the Critical Flow Velocity of Fluid. *Journal of Engineering and Applied Sciences*. 2020 Jan;16(1):98–107.

22. Zhang YL, Gorman DG, Reese JM. Analysis of the vibration of pipes conveying fluid. Proceedings of the Institution of Mechanical Engineers, Part C: *Journal of Mechanical Engineering Science*. 1999 Aug 1;213(8):849–59.

23. Sugiyama Y, Tanaka Y, Kishi T, Kawagoe H. Effect of a spring support on the stability of pipes conveying fluid. *Journal of Sound and Vibration*. 1985 May;100(2):257–70.

24. Lee U, Oh H. The spectral element model for pipelines conveying internal steady flow. *Engineering Structures.* 2003 Jul;25(8):1045–55.

25. Lee U, Jang I, Go H. Stability and dynamic analysis of oil pipelines by using spectral element method. *Journal of Loss Prevention in the Process Industries*. 2009 Nov;22(6):873–8.

26. Gorman DG, Reese JM, Zhang YL. Vibration Of A Flexible Pipe Conveying Viscous Pulsating Fluid Flow. *Journal of Sound and Vibration*. 2000 Feb;230(2):379–92.

27. Schwer LE. An Overview of the ASME V&V-10 Guide for Verification and Validation in Computational Solid Mechanics. In Espoo, Finland: SMiRT 20-Division 3; 2009. p. 1–10. (Paper 2010).

28. Li S jun, Liu G min, Kong W tao. Vibration analysis of pipes conveying fluid by transfer matrix method. *Nuclear Engineering and Design*. 2014 Jan;266:78–88.

APPENDIX A : MATLAB program Computing Natural Frequencies

```
% Program for finding the 1st and 2nd natural frequencies for flow
% induced vibrations in piping using finite difference method for
% the pipe with fixed ends i.e. (clamped-clamped).

clear all;

%% Problem parameters

E=207E9;        % Young's Modulus of Pipe [Pa]
L=3.048;        % Pipe clamp spacing [m]
I = 8.73E-09;   % Moment of Inertia of Pipe [m^4]
mtot = 1.386;   % Total mass of pipe and fluid per unit length [kg/m]
mf = 0.38;      % Mass of fluid per unit length [kg/m]
V = 50;         % Fluid Velocity [m/s]

%% Discretisation of the pipe
Nx=60;          % Number of spatial grid points (i=1 at x=0; i=Nx at x=L)
deltax=L/(Nx-1);% Spatial grid spacing

%% Defining the constants for the set of linear finite difference equations

a = (E*I)/(mtot*deltax^4);
b = (mf*V^2)/(mtot*deltax^2);

C1 = a;
C2 = b-4*a;
C3 = 6*a-2*b;
C4 = b-4*a;
C5 = a;

%% Creation of FDM Matrix M
n = Nx-2;       %Defines size of matrix
M = zeros(n);

M(1,1)= C1+C3;
M(1,2)= C4;
M(1,3)= C5;

M(2,1)= C2;
M(2,2)= C3;
M(2,3)= C4;
M(2,4)= C5;

for k =3:n-2
    M(k,k-2)=C1;
    M(k,k-1)=C2;
    M(k,k)=C3;
    M(k,k+1)=C4;
    M(k,k+2)=C5;
end

M(n-1,n-3)= C1;
M(n-1,n-2)= C2;
```

```
M(n-1,n-1)= C3;
M(n-1,n)= C4;

M(n,n-2)= C1;
M(n,n-1)= C2;
M(n,n)= C3+C5;

%% Calculating the set of natural frequencies from the eigen values of M
W = sqrt(eig(M));   %Computes the vector of natural frequencies from the
                    %vector of eigen values
W_real = real(W);   %Takes the real parts of the natural frequency

w_natural1 = W_real(1) %Extracts the 1st Natural Frequency
w_natural2 = W_real(2) %Extracts the 2nd Natural Frequency

%Displaying Results in Command Window
X1 = ['1st Natural Frequency = ',num2str(w_natural1),' rad/s.'];
disp(X1)
X2 = ['2st Natural Frequency = ',num2str(w_natural2),' rad/s.'];
disp(X2)
```

APPENDIX B : MATLAB program Computing Critical Velocity

```
% Program for finding the Critical Velocity for flow
% induced vibrations in piping using finite difference method for
% the pipe with fixed ends i.e. (clamped-clamped).

% Program utilises a 3 stage search step reducing root finding algorithm
% to efficiently find the fluid velocity where the natural frequency where
% the natural frequency becomes zero and without complex parts.

clear all;

%% Problem parameters

E=207E9;        % Young's Modulus of Pipe [Pa]
L=3.048;        % Pipe clamp spacing [m]
I = 8.73E-09;   % Moment of Inertia of Pipe [m^4]
mtot = 1.386;   % Total mass of pipe and fluid per unit length [kg/m]
mf = 0.38;      % Mass of fluid per unit length [kg/m]


%% Discretisation of the pipe
Nx=60;          % Number of spatial grid points (i=1 at x=0; i=Nx at x=L)
deltax=L/(Nx-1);% Spatial grid spacing

%% 1ST STAGE SEARCH
% Calculates the Natural Frequency at Fluid Velocity Intervals of 10m/s
% At every step checks whether the natural frequencies are still real
% Search stops when the vector of natural frequencies has a complex
% component and the last velocity with a real natural frequency is computed
% used in the next stage of search

V = 1;
W(1) = 1;

while  W == real(W)

% Defining the constants for the finite difference equations

a = (E*I)/(mtot*deltax^4);
b = (mf*V^2)/(mtot*deltax^2);

C1 = a;
C2 = b-4*a;
C3 = 6*a-2*b;
C4 = b-4*a;
C5 = a;

% Creation of FDM Matrix M
n = Nx-2;
M = zeros(n);

M(1,1)= C1+C3;
M(1,2)= C4;
M(1,3)= C5;

M(2,1)= C2;
```

```
M(2,2)= C3;
M(2,3)= C4;
M(2,4)= C5;

for k =3:n-2
    M(k,k-2)=C1;
    M(k,k-1)=C2;
    M(k,k)=C3;
    M(k,k+1)=C4;
    M(k,k+2)=C5;
end

M(n-1,n-3)= C1;
M(n-1,n-2)= C2;
M(n-1,n-1)= C3;
M(n-1,n)= C4;

M(n,n-2)= C1;
M(n,n-1)= C2;
M(n,n)= C3+C5;

% Calculating the set of natural frequencies from the eigen values of M
W = sqrt(eig(M));
V = V + 10;
end

V = V - 20; % stores the velocity where the last real natural
            %  frequency was obtained
W(1) = 1;   %Reinitialises the 1st natural frequency for the next
            % stage of search

%% 2ND STAGE SEARCH
% Similar to stage 1 search but search steps reduced to 1m/s

while  W == real(W)

% Defining the constants for the finite difference equations

a = (E*I)/(mtot*deltax^4);
b = (mf*V^2)/(mtot*deltax^2);
C1 = a;
C2 = b-4*a;
C3 = 6*a-2*b;
C4 = b-4*a;
C5 = a;

% Creation of FDM Matrix M
n = Nx-2;
M = zeros(n);
M(1,1)= C1+C3;
M(1,2)= C4;
M(1,3)= C5;

M(2,1)= C2;
M(2,2)= C3;
M(2,3)= C4;
M(2,4)= C5;

for k =3:n-2
```

```
    M(k,k-2)=C1;
    M(k,k-1)=C2;
    M(k,k)=C3;
    M(k,k+1)=C4;
    M(k,k+2)=C5;
end

M(n-1,n-3)= C1;
M(n-1,n-2)= C2;
M(n-1,n-1)= C3;
M(n-1,n)= C4;
M(n,n-2)= C1;
M(n,n-1)= C2;
M(n,n)= C3+C5;

% Calculating the set of natural frequencies from the eigen values of M
W = sqrt(eig(M));
V = V + 1;
end

V = V - 2; % stores the velocity where the last real natural
            %  frequency was obtained
W(1) = 1;   %Reinitialises the 1st natural frequency for the next
            % stage of search

%% 3RD STAGE SEARCH
% Similar to stage 2 search but search steps reduced to 0.01m/s

while  W == real(W)

% Defining the constants for the finite difference equations
a = (E*I)/(mtot*deltax^4);
b = (mf*V^2)/(mtot*deltax^2);
C1 = a;
C2 = b-4*a;
C3 = 6*a-2*b;
C4 = b-4*a;
C5 = a;

%% Creation of FDM Matrix M
n = Nx-2;
M = zeros(n);

M(1,1)= C1+C3;
M(1,2)= C4;
M(1,3)= C5;
M(2,1)= C2;
M(2,2)= C3;
M(2,3)= C4;
M(2,4)= C5;

for k =3:n-2
    M(k,k-2)=C1;
    M(k,k-1)=C2;
    M(k,k)=C3;
    M(k,k+1)=C4;
    M(k,k+2)=C5;
end
```

```
M(n-1,n-3)= C1;
M(n-1,n-2)= C2;
M(n-1,n-1)= C3;
M(n-1,n)= C4;
M(n,n-2)= C1;
M(n,n-1)= C2;
M(n,n)= C3+C5;

% Calculating the set of natural frequencies from the eigen values of M
W = sqrt(eig(M));
V = V + 0.01;
end

V_crit = V - 0.02; %Computes the final Critical Velocity

%Displaying Results in Command Window
X = ['Critical Velocity = ',num2str(V_crit),' m/s.'];
disp(X)
```

APPENDIX C : MATLAB program Computing Displacements and Amplitude

```
% Program for solving the Flow Induced Vibrations equation for the
% peak displacement along the pipe using finite difference method for
% the pipe with fixed ends i.e. (clamped-clamped).

% Solves d^2y/dt^2 = -(EI/mtot)d^4y/dx^4 - (mf*V^2)d^4y/dx^4 for
% 0 <= x <=L, subject to boundary conditions for the clamped-clamped
% Case which are y(0,t)=y(L,t)=0; dy/dx(0,t)=dy/dx(L,t)=0;
% and also subject to the initial condition dy/dt(x,0)=f(x)

clear all;

%% Problem parameters

E=207E9;        % Young's Modulus of Pipe [Pa]
L=3.048;        % Pipe clamp spacing [m]
I = 8.73E-09;   % Moment of Inertia of Pipe [m^4]
mtot = 1.386;   % Total mass of pipe and fluid per unit length [kg/m]
mf = 0.38;      % Mass of fluid per unit length [kg/m]
V = 50;         % Fluid Velocity [m/s]

u = 0.012;      % Peak vibration velocity [m/s] NB: When analysing a
                % pipeline in operation the value must be measured with
                % vibrometer

%% Discretisation of the pipe
Nx=60;      % Number of spatial grid points (i=1 at x=0; i=Nx at x=L)
deltax=L/(Nx-1); % Spatial grid spacing

%% Computation of free vibration frequency

% Defining the constants for the set of linear FD equations
a = (E*I)/(mtot*deltax^4);
b = (mf*V^2)/(mtot*deltax^2);

C1 = a;
C2 = b-4*a;
C3 = 6*a-2*b;
C4 = b-4*a;
C5 = a;

% Creation of FDM Matrix M
n = Nx-2;
M = zeros(n);

M(1,1)= C1+C3;
M(1,2)= C4;
M(1,3)= C5;
M(2,1)= C2;
M(2,2)= C3;
M(2,3)= C4;
M(2,4)= C5;

for k =3:n-2
```

```
    M(k,k-2)=C1;
    M(k,k-1)=C2;
    M(k,k)=C3;
    M(k,k+1)=C4;
    M(k,k+2)=C5;
end

M(n-1,n-3)= C1;
M(n-1,n-2)= C2;
M(n-1,n-1)= C3;
M(n-1,n)= C4;
M(n,n-2)= C1;
M(n,n-1)= C2;
M(n,n)= C3+C5;

% Calculating the natural frequency from the eigen values of M
W = sqrt(eig(M));
W_real = real(W);
w = W_real(1);

%% Calculating the simulation time
% Peak displacement occurs at T/4 where T is the period of vibration
end_time = 0.25*2*pi/w;

%% Calculate no. of time steps required to meet the stability criteria
Nt=round((Nx*end_time*sqrt(6*E*I*Nx^2-2*mf*V^2*L^2))/...
    (L^2*sqrt(1.5*mtot))+0.5);

deltat=end_time/(Nt-1);

% Defining the constants to be used for time stepping algorithm
% that computes the displacements
a = (E*I/mtot)*(deltat^2/deltax^4);
b = ((mf*V^2)/mtot)*(deltat^2/deltax^2);

y=zeros(Nx,Nt); % Creates Storage of the solution

% Creating the grid for the initial conditions
x=zeros(Nx,1);
t=zeros(Nt,1);
f=zeros(Nx,1);    % Initial condition y(x,0)
g=zeros(Nx,1);

%% Computation of Displacements using FD algorithms

for i=1:Nx
    x(i)=(L*(i-1))/(Nx-1);
    f(i) = 0;
    y(i,1) = f(i);

    %Implementing equation for the initial conditions
    A = ((384*E*I)/(mtot*L^4))-((8*mf*V^2)/(mtot*L^2));
    g(i) = ((16*u)/(L^4*sqrt(A)))*(x(i)^2*L^2-2*x(i)^3*L+x(i)^4)*w;
end

% Assigning values at the boundary nodes where y=0 for all t
time=0.0;
for j=1:Nt
    t(j)=time;
```

```
    y(1,j)=0;
    y(Nx,j)=0;
    time=time+deltat;
end

% Approximating y at the end of the first time step (j=2)
% for i=2, From boundary conditions y(0,j) = y(2,j)
i=2;
bracket = (4*a-b)*y(i-1,1)+(2-6*a+2*b)*y(i,1)...
          +(4*a-b)*y(i+1,1)-a*y(i+2,1);
y(i,2)=0.5*bracket+deltat*g(i);

%Computing y for the nodes i=3 to Nx-2
for i=3:Nx-2
    bracket = -a*y(i-2,1)+(4*a-b)*y(i-1,1)+...
        (2-6*a+2*b)*y(i,1)+(4*a-b)*y(i+1,1)-a*y(i+2,1);
    y(i,2)=0.5*bracket+deltat*g(i);
end

% Approximating y at node i=Nx-1,
% Similarly from boundary condition y(Nx+1,j) = y(Nx-1,j)
i=Nx-1;
bracket = -a*y(i-2,1)+(4*a-b)*y(i-1,1)+(2-7*a+2*b)*y(i,1)...
         +(4*a-b)*y(i+1,1);
y(i,2)=0.5*bracket+deltat*g(i);


% Integrating in time using explicit FD time stepping formula
% j=1 corresponds to the initial conditions at t=0 where y =0
for j=2:Nt-1

    % Computing y at i=2, i=Nx-1 based on boundary conditions
    y(2,j+1) = (4*a-b)*y(1,j)+(2-6*a+2*b)*y(2,j)...
               +(4*a-b)*y(3,j)-a*y(4,j)-y(2,j-1);
    y(Nx-1,j+1) = -a*y(Nx-3,j)+(4*a-b)*y(Nx-2,j)+...
              (2-6*a+2*b)*y(Nx-1,j)+(4*a-b)*y(Nx,j)-y(Nx-1,j-1);

    for i=3:Nx-2
        bracket = -a*y(i-2,j)+(4*a-b)*y(i-1,j)+...
        (2-6*a+2*b)*y(i,j)+(4*a-b)*y(i+1,j)-a*y(i+2,j);
        y(i,j+1) = bracket - y(i,j-1);
    end
end

%% Results
%Plotting of results
for n=Nt
plot(x/L, 1000*y(:,n), 'b', LineWidth=1.2); hold on;
legend('Finite Difference Solution');
xlim([x(1)/L, x(end)/L]);
xlabel('x/L','FontWeight','bold');
ylabel('Peak Displacement (mm)','FontWeight','bold');
grid on;
drawnow;
end

%Calculating the amplitude of vibration. Highest peak displacement
% is the amplitude of vibration.Occurs at the midspan of the pipe
```

```
y_max = 1000*max(max(y));

%Displaying Amplitude and Frequency in Command Window
X1 = ['Vibration Peak Amplitude = ',num2str(y_max),' mm.'];
disp(X1)
X2 = ['Natural Frequency = ',num2str(w),' rad/s.'];
disp(X2)
```

APPENDIX D : Stability analysis of the Finite Difference model

The table below shows the results of the empirical investigation of the stability criterion

No of Spatial Nodes	No of Time Steps	Value of y_{i+1}^{j} coefficient	Model Stability
50	9	**1.6939**	Unstable
90	30	**1.4858**	Unstable
50	10	**1.3384**	Unstable
100	40	**1.2637**	Unstable
90	35	**1.0810**	Unstable
100	44	**1.0395**	Unstable
101	45	**1.0339**	Unstable
150	100	**1.0172**	Unstable
200	179	**1.0049**	Unstable
200	180	**0.9937**	Stable
101	46	**0.9885**	Stable
90	37	**0.9642**	Stable
90	40	**0.8216**	Stable
80	36	**0.6291**	Stable
90	50	**0.5204**	Stable
70	36	**0.3626**	Stable
50	20	**0.3003**	Stable
90	100	**0.1275**	Stable
50	30	**0.1289**	Stable

Coefficient of $y_{i+1}^{j} = \frac{4EI(\Delta t)^2}{m_{total}(\Delta x)^4} - \frac{m_f V^2 (\Delta t)^2}{(\Delta x)^2}$

The model was stable only when the coefficient was less than one. Therefore it was concluded that the stability condition must be

$$\frac{4EI(\Delta t)^2}{m_{total}(\Delta x)^4} - \frac{m_f V^2 (\Delta t)^2}{(\Delta x)^2} < 1$$

APPENDIX E : Simulation Results used to create surrogate model

x1	x2	I	E	mp	mf	mtot	EI	mf /mtot	Vcrit
0.872	0.000	8.73E-09	2.01E+11	0.985	0.052	1.037	1756.40	0.050	379.34
0.154	0.590	8.73E-09	4.50E+10	0.985	0.454	1.439	392.32	0.315	60.60
0.231	0.641	8.73E-09	6.17E+10	0.985	0.504	1.489	538.46	0.338	67.37
0.615	0.359	8.73E-09	1.45E+11	0.985	0.264	1.250	1269.22	0.212	142.83
0.795	0.615	8.73E-09	1.85E+11	0.985	0.479	1.464	1610.25	0.327	119.56
0.487	0.077	8.73E-09	1.18E+11	0.985	0.091	1.076	1025.64	0.085	218.74
0.462	0.282	8.73E-09	1.12E+11	0.985	0.212	1.197	976.93	0.177	139.99
0.103	0.744	8.73E-09	3.38E+10	0.985	0.616	1.601	294.86	0.385	45.10
0.256	0.949	8.73E-09	6.73E+10	0.985	0.898	1.884	587.18	0.477	52.70
0.641	0.769	8.73E-09	1.51E+11	0.985	0.646	1.632	1317.96	0.396	93.07
0.564	0.179	8.73E-09	1.34E+11	0.985	0.148	1.134	1171.79	0.131	183.26
0.846	0.718	8.73E-09	1.96E+11	0.985	0.586	1.572	1707.69	0.373	111.24
0.667	0.256	8.73E-09	1.57E+11	0.985	0.195	1.181	1366.67	0.165	172.45
0.282	0.333	8.73E-09	7.29E+10	0.985	0.246	1.232	635.90	0.200	104.73
0.897	0.231	8.73E-09	2.07E+11	0.985	0.179	1.164	1805.14	0.154	206.91
0.821	0.923	8.73E-09	1.90E+11	0.985	0.858	1.843	1658.97	0.465	90.65
0.333	0.846	8.73E-09	8.40E+10	0.985	0.746	1.731	733.33	0.431	64.64
0.205	0.513	8.73E-09	5.61E+10	0.985	0.385	1.370	489.75	0.281	73.55
0.308	0.154	8.73E-09	7.85E+10	0.985	0.133	1.119	684.61	0.119	147.67
0.692	0.487	8.73E-09	1.62E+11	0.985	0.363	1.348	1415.39	0.269	128.71
0.513	0.872	8.73E-09	1.23E+11	0.985	0.781	1.767	1074.36	0.442	76.43
0.744	0.821	8.73E-09	1.73E+11	0.985	0.711	1.697	1512.82	0.419	95.06
0.974	0.436	8.73E-09	2.24E+11	0.985	0.322	1.307	1951.28	0.246	160.52
0.410	0.974	8.73E-09	1.01E+11	0.985	0.941	1.926	879.49	0.488	63.02
0.179	0.128	8.73E-09	5.05E+10	0.985	0.119	1.104	441.03	0.108	125.53
0.026	0.051	8.73E-09	1.70E+10	0.985	0.078	1.063	148.72	0.073	90.19
0.359	0.538	8.73E-09	8.96E+10	0.985	0.407	1.392	782.04	0.292	90.36
1.000	0.795	8.73E-09	2.29E+11	0.985	0.678	1.663	2000.00	0.408	111.93
0.385	0.410	8.73E-09	9.52E+10	0.985	0.302	1.287	830.78	0.235	108.10
0.128	0.385	8.73E-09	3.94E+10	0.985	0.283	1.268	343.60	0.223	71.83
0.000	0.564	8.73E-09	1.15E+10	0.985	0.430	1.415	100.00	0.304	31.43
0.436	0.692	8.73E-09	1.06E+11	0.985	0.558	1.543	928.21	0.362	84.07
0.923	0.667	8.73E-09	2.12E+11	0.985	0.531	1.516	1853.85	0.350	121.84
0.590	0.026	8.73E-09	1.40E+11	0.985	0.065	1.050	1220.51	0.062	283.30
0.538	0.462	8.73E-09	1.29E+11	0.985	0.342	1.327	1123.07	0.258	118.11
0.769	0.308	8.73E-09	1.79E+11	0.985	0.229	1.214	1561.54	0.188	170.28
0.051	1.000	8.73E-09	2.26E+10	0.985	0.985	1.971	197.43	0.500	29.18
0.077	0.205	8.73E-09	2.82E+10	0.985	0.163	1.149	246.15	0.142	79.98
0.949	0.897	8.73E-09	2.18E+11	0.985	0.819	1.804	1902.57	0.454	99.36
0.718	0.103	8.73E-09	1.68E+11	0.985	0.105	1.090	1464.11	0.096	243.61

x1 and x2 are the Design of Experiment factors to ensure effective exploration of the design space

I – moment of inertia (m^4)

E – Young's Modulus (Pa)

mp – mass of pipe /metre (kg/m)

mf – mass of fluid /metre (kg/m)

mtot – mass of pipe and fluid /metre (kg/m)

EI – Flexural rigidity (Pa m^4)

Vcrit – Critical Velocity (m/s)